

T.C.
REPUBLIC OF TURKEY
HACETTEPE UNIVERSITY
GRADUATE SCHOOL OF HEALTH SCIENCES

**Cloning Putative Voltage-Gated Calcium Channel Gene in *Astacus
Leptodactylus* and Determination of Structural and Functional
Properties of Related Protein**

Berk SAĞLAM (MSc.)

**Program of Biophysics
DOCTOR OF PHILOSOPHY THESIS**

ANKARA

2023

T.C.
REPUBLIC OF TURKEY
HACETTEPE UNIVERSITY
GRADUATE SCHOOL OF HEALTH SCIENCES

**Cloning Putative Voltage-Gated Calcium Channel Gene in *Astacus
Leptodactylus* and Determination of Structural and Functional
Properties of Related Protein**

Berk SAĞLAM (MSc.)

**Program of Biophysics
DOCTOR OF PHILOSOPHY THESIS**

**ADVISOR OF THE THESIS
Prof. Dr. Nuhan PURALI**

ANKARA

2023

**Cloning Putative Voltage-Gated Calcium Channel Gene in *Astacus Leptodactylus*
and Determination of Structural and Functional Properties of Related Protein**

Berk SAĞLAM

Supervisor: Prof. Dr. Nuhan PURALI

This thesis study has been approved and accepted as a PhD dissertation in “Biophysics Program” by the assessment committee, whose members are listed below, on 28.07.2023.

Chairman of the Committee: *Prof. Dr. Belma TURAN*
Lokman Hekim University

Member: *Prof. Dr. Özlem UĞUR*
Ankara University

Member: *Prof. Dr. Turgut BAŞTUĞ*
Hacettepe University

Member: *Prof. Dr. A. Ruhi SOYLU*
Hacettepe University

Member: *Assoc. Prof. Dr. Z. Ekim TAŞKIRAN*
Hacettepe University

This dissertation has been approved by the above committee in conformity to the related issues of Hacettepe University Graduate Education and Examination Regulation.

Prof. Müge YEMİŞCİ ÖZKAN, MD, PhD

Director

YAYIMLAMA VE FİKRİ MÜLKİYET HAKLARI BEYANI

Enstitü tarafından onaylanan lisansüstü tezimin/raporumun tamamını veya herhangi bir kısmını, basılı (kağıt) ve elektronik formatta arşivleme ve aşağıda verilen koşullarla kullanıma açma iznini Hacettepe Üniversitesine verdiğimi bildiririm. Bu izinle Üniversiteye verilen kullanım hakları dışındaki tüm fikri mülkiyet haklarım bende kalacak, tezimin tamamının ya da bir bölümünün gelecekteki çalışmalarda (makale, kitap, lisans ve patent vb.) kullanım hakları bana ait olacaktır.

Tezin kendi orijinal çalışmam olduğunu, başkalarının haklarını ihlal etmediğimi ve tezimin tek yetkili sahibi olduğumu beyan ve taahhüt ederim. Tezimde yer alan telif hakkı bulunan ve sahiplerinden yazılı izin alınarak kullanılması zorunlu metinlerin yazılı izin alınarak kullandığımı ve istenildiğinde suretlerini Üniversiteye teslim etmeyi taahhüt ederim.

Yükseköğretim Kurulu tarafından yayınlanan **“Lisansüstü Tezlerin Elektronik Ortamda Toplanması, Düzenlenmesi ve Erişime Açılmasına İlişkin Yönerge”** kapsamında tezim aşağıda belirtilen koşullar haricince YÖK Ulusal Tez Merkezi / H.Ü. Kütüphaneleri Açık Erişim Sisteminde erişime açılır.

- Enstitü / Fakülte yönetim kurulu kararı ile tezimin erişime açılması mezuniyet tarihimden itibaren 2 yıl ertelenmiştir. ⁽¹⁾
- Enstitü / Fakülte yönetim kurulunun gerekçeli kararı ile tezimin erişime açılması mezuniyet tarihimden itibaren ... ay ertelenmiştir. ⁽²⁾
- Tezimle ilgili gizlilik kararı verilmiştir. ⁽³⁾

28 / 07 /2023

Berk SAĞLAM

1“Lisansüstü Tezlerin Elektronik Ortamda Toplanması, Düzenlenmesi ve Erişime Açılmasına İlişkin Yönerge”

- (1) Madde 6. 1. Lisansüstü teze ilgili patent başvurusu yapılması veya patent alma sürecinin devam etmesi durumunda, tez **danışmanın**ın önerisi ve **enstitü anabilim dalının** uygun görüşü üzerine **enstitü** veya **fakülte yönetim kurulu** iki yıl süre ile tezin erişime açılmasının ertelenmesine karar verebilir.
- (2) Madde 6. 2. Yeni teknik, materyal ve metotların kullanıldığı, henüz makaleye dönüşmemiş veya patent gibi yöntemlerle korunmamış ve internette paylaşılması durumunda 3. şahıslara veya kurumlara haksız kazanç imkanı oluşturabilecek bilgi ve bulguları içeren tezler hakkında tez **danışmanın**ın önerisi ve **enstitü anabilim dalının** uygun görüşü üzerine **enstitü** veya **fakülte yönetim kurulunun** gerekçeli kararı ile altı ayı aşmamak üzere tezin erişime açılması engellenebilir.
- (3) Madde 7. 1. Ulusal çıkarları veya güvenliği ilgilendiren, emniyet, istihbarat, savunma ve güvenlik, sağlık vb. konulara ilişkin lisansüstü tezlerle ilgili gizlilik kararı, **tezin yapıldığı kurum** tarafından verilir *. Kurum ve kuruluşlarla yapılan iş birliği protokolü çerçevesinde hazırlanan lisansüstü tezlere ilişkin gizlilik kararı ise, **ilgili kurum ve kuruluşun önerisi** ile **enstitü** veya **fakültenin** uygun görüşü üzerine **üniversite yönetim kurulu** tarafından verilir. Gizlilik kararı verilen tezler Yükseköğretim Kuruluna bildirilir.

Madde 7.2. Gizlilik kararı verilen tezler gizlilik süresince enstitü veya fakülte tarafından gizlilik kuralları çerçevesinde muhafaza edilir, gizlilik kararının kaldırılması halinde Tez Otomasyon Sistemine yüklenir

* Tez **danışmanın**ın önerisi ve **enstitü anabilim dalının** uygun görüşü üzerine **enstitü** veya **fakülte yönetim kurulu tarafından** karar verilir

ETHICAL DECLARATION

In this thesis study, I declare that all the information and documents have been obtained in the base of the academic rules and all audio-visual and written information and results have been presented according to the rules of scientific ethics. I did not do any distortion in data set. In case of using other works, related studies have been fully cited in accordance with the scientific standards. I also declare that my thesis study is original except cited references. It was produced by myself in consultation with supervisor (Prof. Dr. Nuhan PURALI) and written according to the rules of thesis writing of Hacettepe University Institute of Health Sciences.

Berk SAĞLAM

ACKNOWLEDGMENTS

Hereby I present my deepest gratitude for the help and support of following persons during my thesis study.

I would like to thank my advisor Prof. Dr. Nuhan PURALI for his endless support and guidance from the beginning to the end of my thesis study.

Also, I would like to thank Prof. Dr. Turgut BAŞTUĞ, Prof. Dr. A. Ruhi SOYLU, Prof. Dr. Belme TURAN, Prof. Dr. Özlem UĞUR, Assoc. Prof. Dr. Z. Ekim TAŞKIRAN, and Asst. Prof. Nurhan ERBİL for their support during my study.

I deeply appreciate Bora ERGİN, Nazlı COŞKUN BEYATLI, Kaan ARSLAN and Berkay ARSLAN for their support and friendship.

Many thanks should also go to staff of the Biophysics Department for their friendship and their efforts to provide a productive environment.

I would also like to thank to all of my friends, here in Turkey and all over the world, for their valuable support and patience.

I would like to express my deepest appreciation to my parents Prof. Dr. Semran SAĞLAM and Prof. Dr. Necdet SAĞLAM for their limitless love and support, even in dark times.

My final thanks go to my cat Bal Mestan, who didn't care about my PhD at all, which helped tremendously in putting things in perspective for me and made this journey much smoother to sail through.

ABSTRACT

Saglam, B., Cloning Putative Voltage-Gated Calcium Channel Gene in *Astacus Leptodactylus* and Determination of Structural and Functional Properties of Related Protein. Hacettepe University Graduate School of Health Sciences, Ph.D. Thesis in Biophysics, Ankara, 2023. Voltage-gated calcium channels are essential elements in development of many cellular processes like electrical signaling, contraction secretion and gene expression. There has been a fair amount of information about the functional and structural properties of the calcium channels in mammalian species. Crayfish serves as a model animal for many types of experiments. However, there has been no information related to the molecular and genetic properties of the calcium channels in the crayfish. Conventional cloning methods, three-dimensional structural calculations, docking experiments have been conducted. An mRNA 7791 bp in size has been cloned. The coding region has been translated into an alpha peptide with 1942 residues. The cloned protein sequence has similarity to other L-type voltage-gated calcium channel sequences from the neighboring species. Three-dimensional structure, in reference to human L-type voltage-gated calcium channel, has been calculated. Known calcium channel blockers; nifedipine, verapamil and diltiazem have been successfully docked on the calculated three-dimensional model. Considering the similarity assay in the NCBI platform, the three-dimensional structural calculations and the docking experiments it was concluded that the cloned mRNA codes an alpha peptide for a putative voltage-gated calcium channel protein in the crayfish. In the present work by using the conventional molecular biology methods complete mRNA coding a putative calcium channel was *de novo* cloned. Three-dimensional structure of the related protein was calculated and several pharmacological agents blocking the channel were docked to the identified receptor sites.

Key words: Cloning, calcium channel, modeling, docking, crayfish

Supported by: Hacettepe University Research Foundation (# 15403, 19942), The Scientific and Technological Research Council of Turkey (# 218S553)

ÖZET

Sağlam, B., *Astacus leptodactylus* Türünde Voltaj Kapılı Kalsiyum Kanalına Ait Genlerinin Klonlanması ve İlgili Proteinlerin Yapısal ve Fonksiyonel Özelliklerinin Belirlenmesi. Hacettepe Üniversitesi Sağlık Bilimleri Enstitüsü Biyofizik Programı Doktora Tezi, Ankara, 2023. Voltaj kapılı kalsiyum kanalları, elektrik sinyali, kasılma salgısı ve gen ifadesi gibi birçok hücrel işlemlerin gerçekleşmesinde temel unsurlardır. Memeli türlerinde kalsiyum kanallarının işlevsel ve yapısal özellikleri hakkında oldukça fazla bilgi bulunmaktadır. Kerevit, birçok deney türü için model hayvan görevi görür. Ancak kerevitlerdeki kalsiyum kanallarının moleküler ve genetik özellikleri ile ilgili herhangi bir bilgi bulunmamaktadır. Konvansiyonel klonlama yöntemleri, üç boyutlu yapısal hesaplar, docking deneyleri yapılmıştır. 7791 bp boyutunda bir mRNA klonlanmıştır. Kodlama bölgesi, 1942 amino asitli bir alfa peptidine çevrilmiştir. Klonlanmış protein sekansı, komşu türlerden gelen diğer L-tipi voltaj kapılı kalsiyum kanalı sekansları ile benzerliğe sahiptir. Üç boyutlu yapı, insan L tipi voltaj kapılı kalsiyum kanalına göre hesaplanmıştır. Bilinen kalsiyum kanal blokerleri; nifedipin, verapamil ve diltiazem, hesaplanan üç boyutlu modele başarıyla bağlandı. NCBI platformundaki benzerlik analizi, üç boyutlu yapısal hesaplamalar ve docking deneyleri göz önüne alındığında, klonlanmış mRNA'nın kerevitte varsayılan voltaj kapılı kalsiyum kanalı proteini için bir alfa peptidi kodladığı sonucuna varıldı. Mevcut çalışmada, geleneksel moleküler biyoloji yöntemleri kullanılarak, varsayılan voltaj kapılı kalsiyum kanalını kodlayan mRNA tam olarak *de novo* klonlanmıştır. İlgili proteinin üç boyutlu yapısı hesaplanmıştır ve kanalı bloke eden birkaç farmakolojik ajan belirlenen reseptör bölgelerine yerleştirilmiştir.

Anahtar Kelimeler: Klonlama, kalsiyum kanalı, modelleme, docking, kerevit

Destekleyen Kuruluşlar: Hacettepe Üniversitesi Araştırmalar Fonu (# 15403, 19942), Türkiye Bilimsel ve Teknolojik Araştırma Kurumu (# 218S553)

TABLE OF CONTENTS

APPROVAL	iii
YAYIMLAMA VE FİKRİ MÜLKİYET HAKLARI BEYANI	iv
ETHICAL DECLARATION	v
ACKNOWLEDGMENTS	vi
ABSTRACT	vii
ÖZET	viii
TABLE OF CONTENTS	ix
ABBREVIATIONS	ix
FIGURES	xiii
TABLES	xv
1. INTRODUCTION	1
2. LITERATURE REVIEW	2
3. MATERIALS AND METHODS	10
3.1. Model Animals	10
3.2. Tissue Extraction from the Model Animal	10
3.3. Total RNA Isolation	10
3.4. cDNA Library Construction	11
3.4.1. cDNA Synthesis by using SMARTer RACE 5' / 3' Kit.	11
3.4.2. cDNA synthesis by using REPLI-g WTA Single Cell Kit	12
3.5. Polymerase Chain Reaction	14
3.5.1. Designing the Primers	14
3.5.2. Procedures for Polymerase Chain Reactions	14
3.6. Gel Electrophoresis of PCR Products	17
3.7. Gel Extraction and PCR Product Purification	17

3.8. Sequencing the Products	18
3.9. Isolation of a1Ic-HE3-pcDNA3 plasmid	19
3.10. Synthesis of cRNA	19
3.11. Harvesting and Defollunication of Oocytes	21
3.12. Transferring cRNA into Selected Oocytes	21
3.13. Electrophysiology and Data Analysis	21
3.14. SWISS-MODEL and Docking in AutoDock	22
4. RESULTS	23
5. DISCUSSION	43
6. CONCLUSION	46
7. REFERENCES	47
8. APPENDIX	54
APPENDIX 1: Thesis Originality Report	
APPENDIX 2: Digital Receipt	
9. CURRICULUM VITAE	56

ABBREVIATIONS

°C	Degree Celsius
Ag	Silver
AgCl	Silver chloride
α	Alpha
Å	Angstrom
β	Beta
bp	Base pair
BTZ	Benzodiazepines
BLAST	Basil local alignment search tool
Ca²⁺	Calcium ion
Ca_v	Voltage-gated calcium channels
CDI	Calcium-dependent inactivation
CDS	Coding Sequence
cDNA	Complementary deoxyribonucleic acid
δ	Delta
dH₂O	Distilled water
DHP	Dihydropyridines
DNA	Deoxyribonucleic acid
dNTP	Deoxy nucleoside triphosphate
DTT	Dithiothreitol
g	g-factor
γ	Gamma
GMQE	Global model quality estimation
HVA	High voltage activated
K⁺	Potassium ion
kbp	Kilobase pair
KCl	Potassium chloride
kDa	kilodalton
LVA	Low voltage activated

mg	Milligram
ml	Milliliter
μl	Microgram
mM	Millimolar
MΩ	Megaohm
mV	Millivolt
mRNA	Messenger ribonucleic acid
Na⁺	Sodium ion
NCBI	National center of biotechnology information
NGS	Next generation sequencing
ORF	Open reading frame
PAA	Phenylalkylamines
PCR	Polymerase chain reaction
QMEAN	Qualitative model energy analysis
RACE	Rapid amplification of cDNA ends
RNA	Ribonucleic acid
RT	Room temperature/Reverse transcriptase
RyR	Ryanodine receptor
T_m	Melting temperature
UPM	Universal Primer Mix
WTA	Whole transcriptome amplification

FIGURES

Figure	Page
2.1. Cellular events triggered by the voltage-gated Ca ²⁺ channels.	2
2.2. Subunit structures of a representative voltage-gated calcium channel (1).	4
2.3 The α 1 subunit of voltage-gated calcium channel.	4
2.4 Phylogeny of α 1 subunits of voltage-gated calcium channels (33).	5
2.5. Calcium binding sites (Sites 1,2,3) of selectivity filter (43).	6
4.1. Image of Gel electrophoresis: Lane 1: 100 bp Ladder. Lane2: CavLk1-F1'/R1' PCR product. (Template: Muscle). Lane 3: reference (Template: Muscle). Lane 4: Empty Lane. Lane 5: CavLk1-F1'/R1'(Template Ganglion). Lane 6: reference (Template Ganglion).	24
4.2. Image of Gel electrophoresis: Lane 1: Product of the First RACE PCR with TB5R'. Lane 2: Product of nested RACE PCR with TB4R'. Lane 3: 1kbp Ladder.	26
4.3. Image of Gel electrophoresis: Lane 1: 1 kbp Ladder. Lane 2: The product of PCR with CaV22L3f and CaVhaL1r	27
4.4. Image of Gel electrophoresis: Lane 1: 1 kbp Ladder. Lane 2: The product of RACE PCR with CaVm31R4f4. Lane 3: The product of nested RACE PCR with CaVm31R4f5.	30
4.5. Image of Gel electrophoresis: Lane 1: The product of nested RACE PCR with CaVmCf2. Lane 2: The product of nested RACE PCR with CaVmCf3. Lane 3: 1 kbp Ladder. The image in Right: The extraction of the band from the gel.	31
4.6. Image of Gel electrophoresis: Lane 1: 1 kbp Ladder. Lane 2: The product of RACE PCR with CaV5raceR2. The image in Right: The extraction of the band from the gel.	32
4.7. Image of Gel electrophoresis: Lane 1: 1 kbp Ladder. Lane 2: The product of RACE PCR with CaV3raceF. The image in Right: The extraction of the band from the gel.	33
4.8. Map of the complete sequence (black) with ORF (orange). Alignment of the fragments (grey).	33
4.9. The complete sequence of L-type voltage-gated Calcium Channel.	35
4.10. Map Image of complete sequence and fragments of voltage sensor, ion selectivity filter, DHP binding sites, IQ and GPHH domain.	36
4.11. The results of the analysis done in NCBI Blast with the gene's protein sequence.	36
4.12. The results from NCBI Conserved Domain Database Analysis with the gene's amino acid sequence.	37

- 4.13.** Image of Gel electrophoresis: Lane 1: 1 kbp Ladder. Lane 2: The product of PCR with cavFk1 and cavRk1. 38
- 4.14.** Successful alignments of short reads with sequence of the gene. 38
- 4.15.** The phylogenetic tree analysis for cloned channel. 39
- 4.16.** 3D Structures of the cloned channel by Swiss-Model. A: 3D structure of channel in VMD'S cartoon mode (83). B: 3D structure of the protein in membrane by MEMEMBED Prediciton, PSIPRED, UCL (84). 40
- 4.17.** Voltage sensor (purple), selectivity filter (green) and DHP receptor (red) regions are shown in A, B and C, respectively. 40
- 4.18.** Docking of diltiazem, nifedipine and verapamil molecules (yellow) to the cloned channel protein, A, B and C respectively. Green and red segments are the selectivity filters and DHP binding sites, respectively. 41
- 4.19.** Calcium currents from calcium channel plasmid (a1Ic-HE3-pcDNA3) injected oocytes. A: voltage clamp steps. B: Evoked current responses. C: current-voltage relationship. 42
- 5.1.** The Amino Acid Sequence of cloned voltage-gated Calcium Channel. Voltage sensors highlighted in purple, selectivity filter in green, IQ and GPHH domains in blue and DHP receptor sites colored in red. 43

TABLES

Table	Page
3.1. Buffer mixture solution for both 5' and 3' reactions.	11
3.2. Mixture solution for preparation of 5' cDNA synthesis and 3' cDNA synthesis.	11
3.3. Master mixture solutions for both 5'- and 3'- cDNA synthesis reactions.	12
3.4. Reaction mixture of cDNA synthesis by using REPLI-g WTA Single Cell Kit.	12
3.5. Quantiscript RT mixture.	13
3.6. Ligation mixture	13
3.7. REPLI-g SensiPhi mixture.	13
3.8. OneTaq Quick-Load DNA Polymerase's Reaction mixture.	15
3.9. OneTaq Quick-Load DNA Polymerase's Conditions of Thermal Cyclers.	15
3.10. Reaction mix for Platinum SuperFi II DNA Polymerase.	15
3.11. Conditions of Thermal Cycling for Platinum SuperFi II DNA Polymerase.	16
3.12. SeqAmp PCR Master Mixture.	16
3.13. Reaction mixture for 5'- and 3'-RACE reactions.	16
3.14. Conditions of Thermal Cycling for SeqAmp DNA Polymerase.	17
3.15. The mixture for BigDye Terminator Cycle Sequencing Kit	18
3.16. Conditions of Thermal Cycling for BigDye Terminator Cycle Sequencing Kit	18
3.17. Reaction Mixture for Linearization	20
3.18. RNA synthesis mixture.	20
4.1. L-type Voltage-gated Calcium Channel mRNA sequences of closely related species for obtaining consensus sequence.	23
4.2. Primers used in the first successful PCR.	24
4.3. Primers used in the first RACE_PCR Experiment.	25
4.4. Primers from Fragment-1.	26
4.5. Primers from Fragment-2.	27
4.6. Repeat motifs related to ion selectivity.	28
4.7. Degenerate primers from 3rd and 4th repeat motifs of Scylla paramamosain's L-type Ca _v	28
4.8. Primers from Fragment-3.	29
4.9. Repeat sequences related voltage sensor.	29
4.10. Primers from voltage sensor's repeat motifs and conserved domains.	29

4.11. Primers from Fragment-4.	31
4.12. Primers for final RACE PCR experiments.	32
4.13. Primers for obtaining complete sequence of the gene.	37
5.1. Ion selectivity domain motifs.	44
5.2. Voltage sensor domain motifs.	44
5.3. DHP Binding sites.	45

1. INTRODUCTION

Voltage-gated calcium channels (Ca_v), gated by potential changes in the cell membrane, generate a Ca^{2+} influx acting as a second messenger for many important cellular processes like muscle activity, secretion, and gene transcription (1).

Astacus leptodactylus is a very useful model animal for many types of experiments. Due to the simplified morphology and relative ease in access to the neural circuitry it is particularly convenient for many neuroscience studies. The electrical and functional properties of the many types of cells almost have completely been investigated. (2-7). In comparison to the functional studies amount of information about the genetic properties of the animal is rather limited. Recently, several ion channel genes that give cells many essential electrical and functional properties have been explored by our laboratory. mRNAs coding a voltage gated sodium channel, sodium-calcium exchanger, inward rectifier potassium channel, calcium activated potassium channel, ryanodine receptor, transmembrane channel-like protein and Piezo channel have been cloned (8-13). Calcium channels play an important role in the muscle and neural physiology in this model animal. However, there is no information about the genetic and molecular properties of the voltage-gated calcium channels in this model animal.

Therefore, the aim of this study was to clone the voltage-gated calcium channel (Ca_v) of *Astacus leptodactylus* and to examine its electrical and functional properties by computational modeling and heterologous expressing in *Xenopus laevis* oocytes.

2. LITERATURE SEARCH

2.1. Voltage-gated Calcium Channels

Voltage-gated calcium channels (Ca_v) are activated in variety of cell types in response to depolarization and mediate a Ca^{2+} influx acting as a second messenger for electrical signaling and subsequent cellular processes (1). Voltage-gated Ca^{2+} channels have an important role in transducing the changes in membrane potential into a Ca^{2+} influx for physiological processes such as muscle excitability, contraction, secretion, protein phosphorylation, enzyme regulation and gene transcription (Figure 2.1) (1, 14, 15, 16).

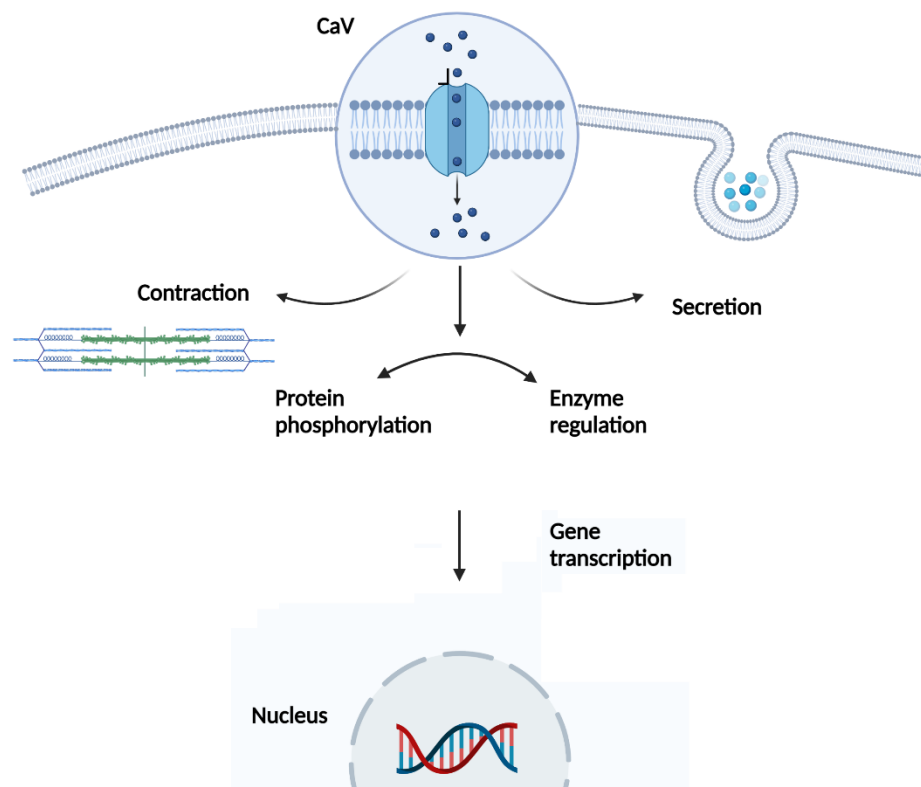


Figure 2.1. Cellular events triggered by the voltage-gated Ca^{2+} channels. (Created with [BioRender.com](https://www.biorender.com).)

A fair amount of information about calcium channels has been compiled in reference to many molecular biology and electrophysiology experiments even in

humans. Fundamental structural and functional properties of the voltage-gated Ca^{2+} channels have been characterized (17). It is worth to note that the voltage-gated calcium channels were firstly discovered in a crustacean muscle simply by a sodium removal from the bath solution. Although there was no sodium in the solution, the muscle cell was still able to produce action potentials (18, 19). Following the initial recording of skeletal muscle Ca^{2+} channels in 1973, extensive studies were conducted to examine the properties of calcium currents in different invertebrate tissues (20, 21). Calcium currents were observed in all excitable cells including mammalian skeletal and cardiac muscle. (22, 23).

A type of Ca^{2+} channel from T-tubules of skeletal muscle was the first to be purified and cloned (24). First impressions that there could be more calcium channels came from a study of starfish eggs. (25). Subsequently, two calcium current components in mammalian sensory neurons were identified based on their biophysical properties (26, 27). In this work by Carbone and Lux, these components were described for the first time using the terms “high-voltage-activated (HVA)” and “low-voltage-activated (LVA)”, showing that the individual channels responsible for producing these current components have different electrical properties. Because of their long-lasting activation, HVA channels were classified as the “L-type channels” that were sensitive to 1,4-dihydropyridines and were discovered in skeletal muscle, heart, smooth muscle, and neurons. (14,28).

It is initially necessary to recognize voltage-gated calcium channels as a principle part of a protein complex. Voltage-gated calcium channel complex, also known as DHP receptor was found to have 5 different components as in skeletal muscle (Figure 2.2). These components are α_1 which is main pore-forming subunit called Ca_v (190 kDa), a disulfide-linked glycoprotein dimer of α_2 (150 kDa) and δ (17–25 kDa), intracellular β (55 kDa) and transmembrane glycoprotein subunit γ (33 kDa), in an approximately equal stoichiometric ratio (29,30).

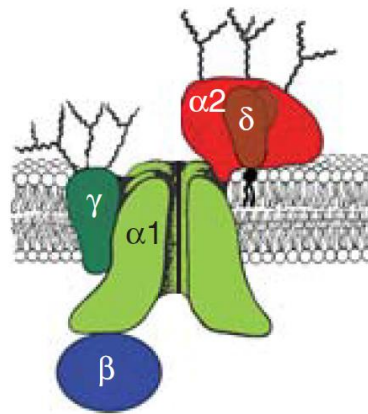


Figure 2.2. Subunit structures of a representative voltage-gated calcium channel. (1).

Although the auxiliary $\alpha 2\delta$ and β subunits of the voltage calcium channel increase the expression of functional channels at the membrane, they are not directly involved in the formation of the selective pore (14). As this is the case, examinations were focused onto the $\alpha 1$ subunit, which is responsible for the pore structure and selectivity. Ca^{2+} , Na^{+} , and K^{+} channels are voltage-gated ion channels that are part of a large multigene protein family termed as 4x6TM (Four copies of a six transmembrane protein domain). The $\alpha 1$ subunit of voltage-gated calcium channel has 24 transmembrane segments, six segments (S1-S6) in each one of four homologous repeats (DI-DIV) (14, 17, 31, 32) (Figure 2.3).

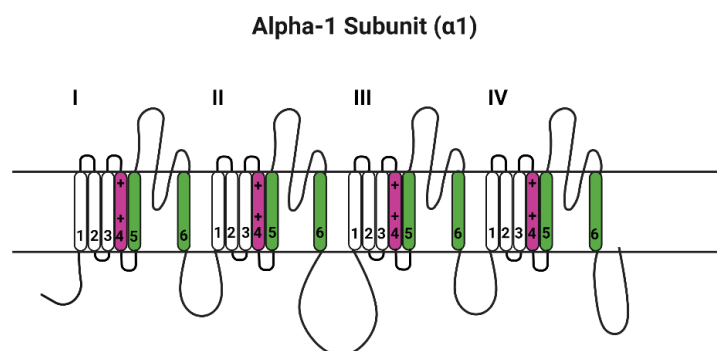


Figure 2.3. The $\alpha 1$ subunit of voltage-gated calcium channel. (Created with BioRender.com.)

Mammalian voltage-gated calcium channels are present in ten different genes (Figure 2.4). The related α 1 units of each gene possess a different function and expression pattern (33).

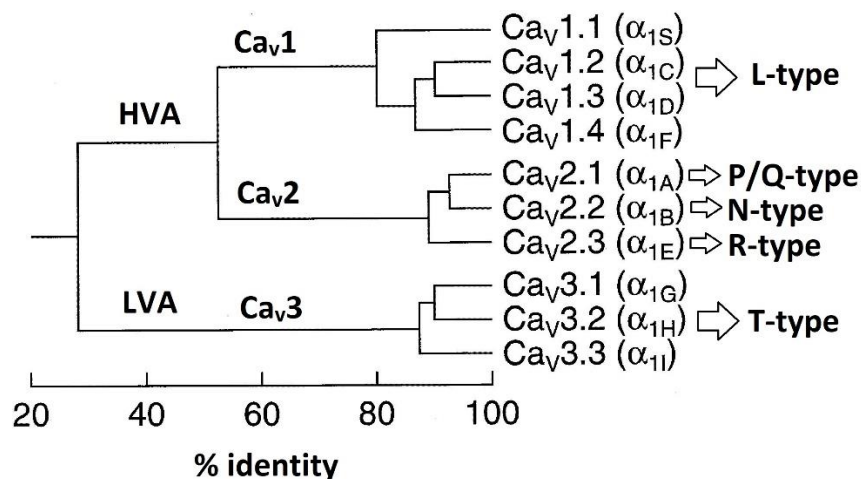


Figure 2.4. Phylogeny of α 1 subunits of voltage-gated calcium channels (33).

The Ca_v1 family consists of 4 different members, each of which is an L-type calcium channel. Ca_v1.1 is an isoform found in skeletal muscle, while Ca_v1.2 is found specifically in cardiac muscle. Ca_v1.3 and 1.4 are activated at low voltage levels and expressed less frequently in cardiac and skeletal muscle cells (34). While the Ca_v1 subfamily is involved in the regulation of contraction, secretion and gene expression in neurons, in special sensory cells it takes part in synaptic transmission (34).

Members of the Ca_v2 subfamily play a major role in initiating synaptic transmission at fast synapses. Ca_v2.1 is defined as P/Q type calcium channels (35) and Ca_v2.2 has the molecular structure similar to the neuronal N type calcium channels (36). Ca_v2.3 channels were found to be more inactivating than other HVA channels (36). However, it may contribute to the R-type calcium current (34). The Ca_v3 subfamily is involved in the rhythmic repetitive firing of action potentials in cardiac myocytes and thalamic neurons. Homology comparisons show that members of the Ca_v3 group are quite different from the HVA channels and are assigned into LVA channels (34, 38).

The $\alpha 1$ subunit of the voltage-gated calcium channel contains 24 transmembrane segments, of which the S1-S4 segment provides voltage sensitivity and the S5-S6 segment forms pore structure (39). In voltage dependent calcium channels, the pore-forming segments S5–S6 and the connecting P loop play a significant role in determining selectivity and conductance. They are highly selective for calcium ion (40). The pore loop at the external end of the channel which is lined with a cluster of negatively charged glutamate residues in each domain, is responsible for Ca^{2+} selectivity (15, 31, 41, 42).

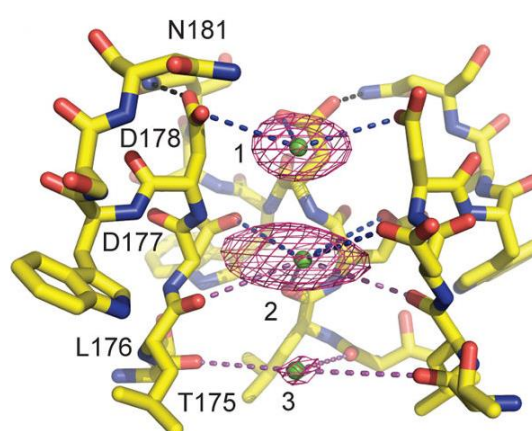


Figure 2.5. Calcium binding sites (Sites 1,2,3) of selectivity filter (43).

In the selectivity filter, three binding sites were discovered and identified as Sites 1,2 and 3 (Figure 2.5). Site 1 has four carboxyl side chains of glutamate and is placed at the mouth of the filter. Site 2 has a single occupancy and is constituted by four carbonyl side chains in addition to four backbone carbonyls. Site 3, which has a lower affinity, is formed only by four backbone carbonyls and facilitates exit into the central cavity (43).

Voltage-gated calcium channels have an important self-regulating mechanism called calcium-dependent inactivation (CDI). A conserved aspartate in Domain II (DII) of the selectivity filter is required for calcium-dependent inactivation (44). A variety of studies have suggested a strong connection between ion selectivity and CDI, based on the observation that selectivity filter mutations, particularly glutamate in the S5-S6 loop of the third and fourth repeats, simultaneously impact calcium dependent

inactivation and selectivity properties (31, 41, 44). The mutation from EEEE to EEQE in the third repeat's S5-S6 loop, which abolishes calcium-dependent inactivation, strongly suggests that the selectivity locus is crucial for calcium-dependent inactivation (15). Moreover, the activation of calcium conductance and calcium-dependent inactivation is influenced by the amount of extracellular calcium concentration (45). The selectivity filter acts as the gateway for calcium-dependent inactivation, wherein this process specifically inhibits Ca^{2+} permeation by stabilizing a state of the selectivity filter with high affinity for Ca^{2+} (46, 47).

The central pore of the channel is surrounded by four voltage-sensitive domains, which link channel opening to changes in membrane potential. These domains detect and respond to fluctuations in membrane potential, regulating the flow of ions through the channel (14). Specific amino acid residues, such as Lysine (K) and Arginine (R), which act as the voltage sensor are located in the S4 segment of the voltage-gated channel. These strategically placed positively charged residues in the S4 segment are crucial for detecting changes in membrane potential (48, 49). The S4 segment's positively charged residues are extremely sensitive to changes in membrane potential and go through conformational changes in response to the changes in the electrical field. Each homologous domain's S4 segments function as a voltage sensor when the cell depolarizes. They move outward and rotate in response to the changes in the electric field, translocating towards the extracellular side of the membrane. This movement of the S4 segments causes the adjacent S5 and S6 segments to change conformation, which ultimately forces the channel pore to open (14, 34, 50, 51).

2.2. Heterologous Expression in Oocytes of *Xenopus laevis*

Xenopus oocytes have been used in many different studies in the 40 years since the first experiment in which their capacity to translate exogenous mRNA was determined (52, 53). *Xenopus* oocytes are a suitable model for heterologous expression experiments with their large size for electrophysiological experiments (54, 55, 56). Oocytes from the *Xenopus laevis*, known as the South African clawed frog,

are frequently used in experiments to examine the functional properties of Ca^{2+} channels. (53).

There are five main advantages to using oocytes in heterologous expression experiments. Firstly, *Xenopus* frogs are easy to maintain for in suitable conditions and oocytes can be easily obtained from frogs with a minor surgical intervention (53). Secondly, completely grown *Xenopus* oocytes are durable and can survive for a long time under in vitro conditions (57). Thirdly, the diameter of the oocytes is approximately 1 millimeter at the stage V and VI, so that the desired RNA can be easily injected into the oocyte by microinjection (58). The oocyte is a non-selective but reliable expression system, ion channels and few prokaryotic channels have been expressed from various eukaryotic organisms (59, 60). Finally, functional tests are much easier to perform and observe, because of their relatively large size (60). The disadvantage of the expression system in oocytes is the variation in the quality of the oocytes as a result of seasonal variability observed in many laboratories (55, 62, 63).

Heterologous expression in *Xenopus* oocytes is a very suitable method particularly for ion channels since the electrophysiological examination is easy. Thus, the benefits of using oocytes prevails the disadvantage.

2.3. Protein-Ligand Docking

There are three main classes of antagonists for the Ca^{2+} channels. The first group consists of dihydropyridines (DHP) with nitrendipine, nifedipine and nimodipine, while benzodiazepines (BTZ) group is including diltiazem and phenylalkylamines (PAA) group is including verapamil (18, 64, 65, 66). Diltiazem and verapamil block the ion channel' pore, while DHP antagonists produce allosteric interactions with the channel molecule and potently blocks the channel (67, 68, 69).

The most frequently used and accurate structure-based computational method that helps us to calculate and analyze the interactions between channels and their agonists and antagonists is molecular docking (70). Computational molecular docking models the structures formed between ligands and large molecules and calculates the free energy levels of their binding. This computation process works on

a ligand and macromolecule with known structure. The docking phase estimates the ligand's binding conformation to the large molecule and the binding free energy value (71). The computational docking is based on to find the appropriate conformational space for the ligand, and to estimate the free binding energy of the structure by using scoring function (72). In summary, computational molecular docking is the model to bind small three-dimensional molecules with a target three-dimensional molecular structure in various positions, conformations, and orientations to get the best fit (73).

3. MATERIALS AND METHODS

3.1. Model Animals

In this study, the model animals (crayfish), collected from lakes of Central Turkey, kept in 18-20 °C fresh water aquarium. Their diet includes carrot and fish given once a week. Female *Xenopus laevis* (African clawed frogs) from a breeder are kept in aquarium filled with fresh water at 19 °C. Their diet includes chicken livers once a week. These animals' oocytes are harvested to use in downstream experiments. In the manipulation of experimental animals, Hacettepe University ethics committee approval was obtained and the guidelines were followed.

3.2. Tissue Extraction from the Model Animal

Intermolt animals were selected and kept on ice for 15 minutes and decapitated immediately. Surgical equipment was sterilized and used in collecting of the muscle tissue samples. The collected tissue samples were stored at -80 °C for RNA isolation.

3.3. Total RNA Isolation

Qiazol Lysis Reagent (Qiagen) was used for the process of the total RNA isolation. 20 mg of muscle tissue sample was grinded and homogenized in 1 ml of Qiazol Lysis Reagent by using single-use pestles. After 5 minutes of incubation at room temperature (RT), 200 µl of chloroform was added to the solution and vortexed robustly for 20 seconds. The solution was centrifuged for 15 minutes at 12,000 g at 4 °C. Upper aqueous phase of the solution was transferred into a clean tube meticulously. 500 µl of isopropanol was added and the solution was vortexed and incubated 10 minutes at RT. The solution was centrifuged for 10 minutes at 12,000 g at 4 °C. The supernatant was removed and the pellet was washed in the tube with 1ml of 75 % ethanol. The sample was centrifuged for 5 minutes at 7,500 g at 4 °C and

the supernatant was removed. The pellet was allowed to rest for drying. The RNA pellet was resuspended in RNase-free water and stored at -80 °C.

3.4. cDNA Library Construction

cDNA Libraries were constructed by using two different WTA construction kits; SMARTer RACE 5'/3' Kit (Clontech) and REPLI-g WTA Single Cell Kit (Qiagen). All cDNA synthesis preparation up to the reverse transcription stage were done in a cold environment either by using ice or a cold block to protect the RNA samples.

3.4.1. cDNA Synthesis by using SMARTer RACE 5' / 3' Kit

By using the SMARTer RACE (Rapid amplification of cDNA ends) 5'/3' Kit, RNA samples were reverse transcribed. Long and GC-rich cDNA library production ability was the reason to choose SMARTer RACE Kit. Buffer mixture solution was prepared, given in Table 3.1, for both 5' and 3' cDNA synthesis reactions.

Table 3.1. Buffer mixture solution for both 5' and 3' reactions.

	Volume (µl)
5X First Strand Buffer	4
DTT (100 mM)	0.5
dNTPs (20 mM)	1
Total volume	5.5

Preparation mixtures were prepared as given in Table 3.2 for 5' and 3' reactions. After the incubation at 72 °C for 3 minutes and 42 °C for 2 minutes, the tubes containing Preparation mixtures were span in brief and 1 µl of SMARTer II A Oligonucleotide was added into 5' cDNA synthesis mixture. Master mixtures were prepared for both 5' and 3' cDNA during the incubation period. (Table 3.3)

Table 3.2. Mixture solution for preparation of 5' cDNA synthesis and 3' cDNA synthesis.

5'- cDNA synthesis		3'- cDNA synthesis	
	Volume (µl)		Volume (µl)

Total RNA (10 ng–1 µg)	1-10	Total RNA (10 ng–1 µg)	1-11
5'-CDS Primer A	1	3'-CDS Primer A	1
Sterile H2O	0-9	Sterile H2O	0-10
Total volume	11	Total volume	12

Table 3.3. Master mixture solutions for both 5'- and 3'- cDNA synthesis reactions.

	Volume (µl)
Buffer Mix	5.5
RNase inhibitor (40 U / µl)	0.5
SMARTScribe Reverse Transcriptase (100 U)	2
Total volume	8

After the incubation in the Preparation mixture solutions, Master mixture solution added both for 5' and 3' cDNA synthesis reactions. Then the mixed solutions were incubated at 42 °C for 1.5 hours and at 70 °C for 10 minutes. The end products were diluted with 10 µl of Tricine-EDTA and stored at -20 °C.

3.4.2. cDNA synthesis by using REPLI-g WTA Single Cell Kit

REPLI-g SensiPhi DNA polymerase, included in the kit, has the ability of Multiple Displacement Amplification. Therefore, the kit is successful in amplifying the whole transcriptome with a neglectable sequence bias and detection of very low-abundance transcripts.

The reaction mixture, given in Table 3.4, was incubated at 95 °C for 3 minutes. 2 µl of Genomic DNA Wipeout Buffer was added and that mixture was incubated at 42 °C for 10 minutes.

Table 3.4. Reaction mixture of cDNA synthesis by using REPLI-g WTA Single Cell Kit.

	Volume (µl)
Total RNA (> 10pg- 100ng)	2
dH2O	6
NA Denaturation Buffer	3

While this incubation was taking place, Quantiscript RT mixture given in Table 3.5 was prepared.

Table 3.5. Quantiscript RT mixture.

	Volume (μl)
RT/Polymerase Buffer	4
Random Primer	1
Oligo dT Primer	1
Quantiscript RT Enzyme Mix	1
Total volume	7

The reaction mixture and 7 μ l of Quantiscript RT mixture were combined and incubated at 42 °C for 1 hour. After the incubation at 95 °C for 3 minutes, the mixture was kept on ice to cool.

Table 3.6. Ligation mixture.

	Volume (μl)
Ligase Buffer	8
Ligase Mix	2
Total volume	10

The ligation mixture, given in Table 3.6, was added into the cooled mixture and incubated at 24 °C for 30 minutes and at 95 °C for additional 5 minutes. After the cooling process on ice, REPLI-g SensiPhi mixture given in Table 3.7 was combined with the cooled mixture and incubated at 30 °C for 2 hours and at 65 °C for 5 minutes. Diluted cDNA samples were stored at -20 °C.

Table 3.7. REPLI-g SensiPhi mixture.

	Volume (μl)
REPLI-g SC Reaction Buffer	29

REPLI-g SensiPhi DNA Polymerase	1
Total volume	30

3.5. Polymerase Chain Reaction

Polymerase Chain Reaction (PCR) is an experimental method that has ability to produce excessive amount of a specific sequence copies by using an enzyme called DNA polymerase (74). In order to generate complete and reliable copies of the interested sequence, designing the primers is the first and most important stage.

In this study, OneTaq DNA polymerase (NEB), Platinum SuperFi II (Thermo Fisher) DNA polymerase and SeqAMP DNA polymerase (Takara) were used. OneTaq DNA polymerase was used for the amplification of sequences less than 2.5 kbp (kilobase pairs) in size, while SuperFi II DNA polymerase was used for sequences longer than 2.5 kbp. SeqAMP DNA polymerase (Takara) was used in 5'/3' RACE PCR for uncovering 5' and 3' ends.

3.5.1. Designing the Primers

Primers are short oligonucleotides, produced synthetically, for PCR experiments. For a successful experiment, designed primers need to be 18-26 bp in size and to have 40-60% GC content. In the 3' end of the primers, there should be a purine nucleotide, G or C. Designed primers' melting temperatures (T_m) should be between 50-64 °C and the difference between paired primers should not exceed 5 °C. In addition, the primers should not have no potency to develop neither a dimer nor a hairpin (75).

For a RACE PCR experiment, primers need to have different features. RACE primers should be 23-28 bp in size, have 50-70% GC content and 65-70 °C T_m . Specifically, RACE primers should not be complementary to 3' end primers which are provided with the kit as UPM and Short UPM. A specific code script developed in MATLAB environment were used to generate the primers from the target sequence.

3.5.2. Procedures for Polymerase Chain Reactions

Throughout of the study, three type of PCR kits were used depending on the amplicon size. All the steps prior to PCR were done on cooled block.

For producing the sequences less than 2.5 kbp, OneTaq Quick-Load DNA polymerase Kit (NEB_M0509L) was used. Reaction mixtures and conditions of thermal cycler were given in Table 3.8 and 3.9.

Table 3.8. OneTaq Quick-Load DNA Polymerase's Reaction mixture.

	Volume (μl)
Nuclease-free dH2O	7.5
OneTaq Quick-Load 2X Master Mix with Standard Buffer	12.5
10 μM Forward Primer	2
10 μM Reverse Primer	2
Template DNA	1
Total volume	25

Table 3.9. OneTaq Quick-Load DNA Polymerase's Conditions of Thermal Cycler.

Steps		Temperature	Duration
Initial denaturation		95 °C	2 minutes
40 cycles	Denaturation	95 °C	20 seconds
	Annealing	55 – 65 °C	20 seconds
	Extension	68 °C	1 minute/kbp
Final extension		68 °C	5 minutes

In order to amplify sequences up to 12 kbp, Platinum SuperFi II Green PCR Master Mix (Thermo Fisher_12369010) was used. SuperFi II DNA polymerase is a high-fidelity and universal primer annealing enzyme. Reaction mixtures and conditions of thermal cycler were given in Table 3.10 and 3.11.

Table 3.10. Reaction mix for Platinum SuperFi II DNA Polymerase.

	Volume (μl)
<i>Nuclease-free dH2O</i>	19

2X Platinum SuperFi II PCR Master Mix	25
Forward Primer (10 μM)	2.5
Reverse Primer (10 μM)	2.5
Template	1
Total volume	50

Table 3.1. Conditions of Thermal Cycling for Platinum SuperFi II DNA Polymerase.

Steps		Temperature	Duration
Initial Denaturation		98 °C	30 seconds
30 cycles	Denaturation	98 °C	20 seconds
	Annealing	60 °C	10 seconds
	Extension	72 °C	1 minute/kbp
Final extension		72 °C	5 minutes
Hold		4 °C	

For amplifying sequences that uncovers 5' and 3' ends, RACE experiments by using SeqAmp DNA polymerase (Takara) were conducted. Reaction mixtures and conditions of thermal cycler were given in Table 3.12, 3.13 and 3.14 are suitable for both 5' or 3' RACE experiment.

Table 3.2. SeqAmp PCR Master Mixture.

	Volume (μl)
PCR-Grade dH₂O	15.5
2X SeqAmp Buffer	25
SeqAmp DNA Polymerase	1
Total volume	41.5

Table 3.3. Reaction mixture for 5'- and 3'-RACE reactions.

	Volume (μl)
5'-/3'-RACE-Ready cDNA	2.5
10X UPM	5
5'/3' Gene Specific Primer	1

SeqAmp PCR Master Mixture	41.5
Total volume	50

Table 3.4. Conditions of Thermal Cycling for SeqAmp DNA Polymerase.

Steps	Temperature	Duration
Initial Denaturation	94 °C	2 minutes
25 cycles	94 °C	30 seconds
	68 °C	30 seconds
	72 °C	1 minute/kbp
Hold	4 °C	

3.6. Gel Electrophoresis of PCR Products

Agarose gel electrophoresis (Elite 200 Wealtec) was used to examine the products of PCR experiments.

1 gram of Agarose (Sigma A9539) and 100ml of 1X TBE Buffer were mixed, the solution was heated in a microwave oven until dissolution was completed. Gel casting tray was built while waiting the cooling process of the solution. 3 µl of Ethidium Bromide (10 mg/ml_SNP BiyoTeknoloji) was added to solution and then the mixture was poured into the gel casting tray. After the agarose was solidified, gel was transferred into electrophoresis tank (Cleaver Scientific) filled with 1X TBE buffer. In the loading part of DNA products into wells of gel, 6X Gel Loading Dye (NEB) were mixed with the products. In order to examine the length of the DNA products, 100 bp or 1 kbp Ladders (NEB) were also transferred into wells. Agarose gel was exposed to electric field with potential of 90-100 mV for 45-60 minutes. For observing the separated DNA products, gel was placed under UV light of (Alphamager EC device, Protein Simple). With the help of the Alphamager EC software on the PC, screenshots of the gel electrophoresis result were saved.

3.7. Gel Extraction and PCR Product Purification

In order to use the PCR products in downstream steps, purification of the sample or extracting from the agarose gel was needed. After the examination of the

gel under the UV light, if the interested lane of the gel had some non-specific bands together with the expected band, then the expected band was removed manually from gel and purified by using Monarch DNA Gel Extraction Kit (NEB). When the product examined under UV has single band without any contaminant non-specific bands, then the PCR product was directly purified by using Monarch PCR&DNA Cleanup Kit (NEB). After the purification, the DNA samples' concentrations were measured by Qubit dsDNA High Sensitivity Assay Kit (Thermo Fisher) and samples were stored at -20 °C for further experiments.

3.8. Sequencing the Products

In this study, two methods of sequencing were utilized. If the purified DNA samples was up to 450 bp, then Sanger Sequencing approach was used. In this method, BigDye Terminator Cycle Sequencing Kit was used. The mixture given in Table 3.15 was prepared, conditions of thermal cycle given in Table 3.16 has been applied.

Table 3.15. The mixture for BigDye Terminator Cycle Sequencing Kit.

	Volume (μl)
dH₂O	5.4
BigDye Reaction Mixture	3
Forward or Reverse Primer (10mM)	0.6
Purified DNA Samples	1
Total volume	10

Table 3.16. Conditions of Thermal Cycling for BigDye Terminator Cycle Sequencing Kit.

Steps	Temperature	Duration
50 cycles	95 °C	20 seconds
	55 °C	25 seconds
	60 °C	4 minutes

When the reaction was done, products were analyzed by using a capillary electrophoresis system (ABI 3130 Applied Biosystems). The electropherogram results was examined by using SnapGene Wiever (GSL Biotech LLC).

For larger sequences, a Next Generation Sequencing (NGS) technology was used. Following fragmenting and tagging of DNA samples with Nextera XT DNA Library Preparation Kit (Illumina), samples were sequenced in Illumina Miseq platform and the results were examined in DNASTAR Software's *de novo* assembly pathways.

The *de novo* assembly calculated a scaffold with contigs. In MATLAB platform (76), contigs were aligned to the reference sequence where the primers were designed and the contigs with the best alignment score were chosen for correcting or extending the reference sequence. Selected contigs and extended reference sequence were submitted to the NCBI BLAST platform (77) for annotation. Moreover, the extended reference sequence was scanned in Conserved Domains Database (78) for identification of the functional regions of sequence. The phylogenetic tree has been constructed in MATLAB environment where distances were calculated by using Jukes-Cantor method

3.9. Isolation of a1Ic-HE3-pcDNA3 plasmid

Bacterial stab containing plasmid a1Ic-HE3-pcDNA3, a gift from Edward Perez-Reyes' Lab (Addgene plasmid #45810), was spread onto an agar plate by using a sterile inoculating loop. After overnight incubation, single colonies were inoculated in LB (Ampicillin, 100 µg/mL). In order to check the size, plasmid was linearized with Sfil (Thermo Fischer Scientific) restriction enzyme. The plasmid DNA was purified by using HiSpeed Plasmid Maxi Kit (Qiagen) and the DNA concentration was measured by using Qubit DNA High Sensitive Assay Kit (Thermo Fisher Scientific).

3.10. Synthesis of cRNA

Plasmid DNA was linearized at 37 °C overnight in the reaction mixture given at Table 3.17.

Table 3.17. Reaction Mixture for Linearization.

	Volume (μl)
dH₂O	2
Plasmid DNA (<1 μg)	3
Buffer CutSMART	5
Restriction Enzyme	1
Total volume	10

For the recovery of the linearized DNA, 0.5 μ l 0.5 M EDTA, 1 μ l 3M Na-Acetate and 20 μ l of ethanol were added to the DNA product. After incubation at -20 °C for 1 hour and centrifugation at top speed for 15 minutes, supernatant was removed and the DNA pellet was resuspended with dH₂O.

The mMESSAGE mMACHINE T7 Transcription Kit (Thermo Fisher Scientific) was used for capped cRNA synthesis. Mixture given in Table 3.18 was incubated with DNA product at 37 °C for 2 hours. 1 μ l of TURBO RNase free DNase (Thermo Fisher Scientific) was added and the mixture was incubated at 37 °C for 15 minutes.

Table 3.18. RNA synthesis mixture.

	Volume (μl)
2xNTP/CAP	10
10xBuffer	2
Plasmid DNA	2
dH₂O	3
Enzyme Mix	2
Total	20

30 μ l of RNase free water and 30 μ l of 7.5 M LiCl were added to the mixture and then the mixture was kept at -20 °C for 30 minutes and centrifuged at top speed at 4 °C for 15 minutes. After removing the supernatant, RNA pellet was cleaned with 70% ethanol and resuspended with RNase free water. Concentrations of the RNA product was measured by using Qubit RNA High Sensitive Assay Kit (Thermo Fisher

Scientific) and cRNA products were aliquoted and stored at -80 °C for downstream experiments.

3.11. Harvesting and Defolliculation of Oocytes

After the anesthetizing of *Xenopus laevis* frogs in the solution of 1 g/L MS-222 (Sigma) at 19 °C for 30 minutes, harvested oocytes were kept in Barth's solution prepared with 88 mM NaCl, 2.4 mM NaHCO₃, 1 mM KCl, 0.33 mM Ca (NO₃)₂ * 4 H₂O, 0.41 mM CaCl₂ * 2 H₂O, 0.82 mM MgSO₄ * 7 H₂O, 5 mM Tris HCl for pH 7.4. After the operation of frogs for harvesting oocytes, they kept in isolation. After 2 weeks the sutures were removed.

In order to remove the layer of follicles around the oocytes, 1.5 mg/ml Collagenase was mixed with calcium-free Barth's solution. Oocytes were incubated at 22 °C for 2 hours with shaking. After selecting the stage IV oocytes under microscope, they were kept in Barth's solution.

3.12. Transferring cRNA into Selected Oocytes

Micropipettes, used for injection, were prepared by using Pipette Puller (Sutter P-1000, USA and Narishige PC-100, Japan). Pipettes were filled with diluted cRNA products and were inserted into oocytes with care under microscope. The injection was done by using pressure pulses from a pneumatic micro pump (Pico Spitzer, USA). The injected oocytes kept in 19 °C for a day at least before the downstream experiments.

3.13. Electrophysiology and Data Analysis

Visually selected oocytes were transferred into a recording chamber perfused with a physiological saline (Barth's). Membrane currents of the cRNA injected and WT oocytes were recorded with two electrode voltage clamp method (81). Glass pipettes with 1.5 mm outer and 1.17 mm inner diameter were pulled in a Pipette Puller. Potential recording electrodes had a resistance of 3-5 MΩ and current injecting electrode had a resistance of 1-1.5 MΩ. Both of the electrodes were filled with 3M KCl solution and an Ag-AgCl electrode placed in the bathing medium was

used as reference. Recordings were analyzed and compared between the test and control groups.

3.14. SWISS-MODEL and Docking in AutoDock

The nucleic acid sequence of the CDS region was translated to amino acid sequence and submitted to Swiss-Model platform (Biozentrum University of Basel, Switzerland) for three-dimensional structure calculations [82]. The relevancy of the calculations was evaluated by using the obtained GMQE=0.5 and QMEANDisCo Global=0.65±0.05 values. VMD software was used to view and analyze the calculated 3D structure [83].

Interactions between ligand and the channel were investigated in docking simulations, performed by using AutoDock 4.2.6. AutoGrid program. A grid map in a defined volume of 126 x 98 x 126 xyz points was used in the calculations. Grid spacing was set to 0.375 Å and grid center was designated at dimensions (x, y, and z): 156.162, 168.813 and 161.227. The grid space was chosen as to include the binding site and the selectivity filter of the protein. For each complex 1000 docking experiments were performed using the Lamarckian genetic algorithm with the default parameters except “maximum number for evals” which is set to “long”. During the docking procedure, both the protein and ligands are considered as rigid. The results less than 2.0 Å in positional root-mean-square deviation (RMSD) was clustered together and represented by the result with the most favorable free energy of binding and the highest number of conformations.

4. RESULTS

In the present an mRNA coding a putative calcium channel has been *de novo* cloned. A collection of 15 mRNA sequences from closely related species has been aligned to define a conserved sequence for primer design (Table 4.1).

Table 4.1. L-type Voltage-gated Calcium Channel mRNA sequences of closely related species for obtaining consensus sequence.

<i>Astacus astacus</i>		
	Contig#	Annotation
1	GEDF01015270.1	voltage-dependent calcium channel type D subunit alpha-1
2	GEDF01017322.1	calcium release-activated calcium channel 1 isoform X3
3	GEDF01017323.1	calcium release-activated calcium channel 1 isoform X3
4	GEDF01017324.1	calcium release-activated calcium channel 1 isoform X3
5	GEDF01017325.1	calcium release-activated calcium channel 1 isoform X3
6	GEDF01023835.1	two pore calcium channel 1 isoform X1
7	GEDF01023836.1	two pore calcium channel 1
8	GEDF01023837.1	two pore calcium channel 1
9	GEDF01036364.1	voltage-dependent calcium channel subunit alpha-2 delta-1-like isoform X3
<i>Cancer borealis</i>		
10	JN809809	L-type high-voltage-activated (HVA) calcium
11	JN809808	P/Q-N high-voltage-activated (HVA) calcium
12	JN809810	T-type low-voltage-activated (LVA) calcium
<i>Homarus americanus</i>		
13	KU702651	L-type high-voltage-activated (HVA) calcium
14	KU702650	P/Q-N high-voltage-activated (HVA) calcium
15	KU702652	T-type low-voltage-activated (LVA) calcium

In a previous study, transcriptome drafts for muscle and ganglia tissue were constructed. The consensus/reference sequence were aligned to each one of the transcripts in the transcriptome libraries. The maximum alignment score was with the contig #74313 in Muscle. This contig were examined in NCBI Blast platform and had good alignment with voltage-gated Calcium channel sequences of closely related

species. Aforementioned reference sequence was changed from consensus sequence to contig #74313. Primers given in Table 4.2 were designed on the reference sequence.

Table 4.2. Primers used in the first successful PCR.

Name of the Primer	Sequence 5'→3'
CavLk1_R1'	TTCTTCGTGGTGCTGTTTACATGTG
CavLk1_F1'	GGTTCGATGTGAAGGCCCTAAGAGC

Primers were used in PCR experiments. PCR with muscle template was successful and produced approximately 600 bp band (Figure 4.1). The band was extracted from the gel and purified then sequenced by Sanger Sequencing method. Obtained sequence was 416 bp long and were aligned on NCBI Blast. The maximum alignment score was with "*Homerus americanus* voltage-dependent L-type Calcium channel alpha-1 subunit mRNA" and this result confirmed the partial Sanger Sequence that the fragment should belong to a voltage-gated calcium channel mRNA.

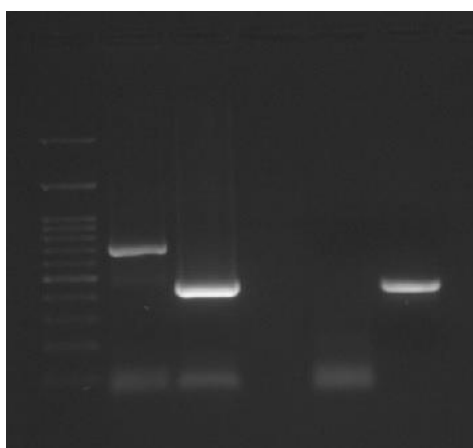


Figure 4.1. Image of Gel electrophoresis: Lane 1: 100 bp Ladder. Lane2: CavLk1-F1'/R1' PCR product. (Template: Muscle). Lane 3: reference (Template: Muscle). Lane 4: Empty Lane. Lane 5: CavLk1-F1'/R1'(Template Ganglion). Lane 6: reference (Template Ganglion).

RACE primers given in Table 4.3 were designed from the partial Sanger Sequence to reveal the 5' and 3' regions. Prior to the RACE PCR experiment, the primers were paired appropriately with each other and their efficiencies were tested.

TB8F'/TB5'R pairs was successful. The PCR product was Sanger sequenced. It was observed the sequence matched with the reference sequence.

Table 4.3. Primers used in the first RACE_PCR Experiment.

Name of the Primer	Sequence 5'→3'
TB1R'	GCTTCCAAGGCTACTTTGTATCACTG
TB1F'	CAGTGATACAAAGTAGCCTTGGAAGC
TB2F'	GTGATACAAAGTAGCCTTGGAAGCCT
TB3R'	CAGTTTAGGCTTCCAAGGCTACTTTG
TB4R'	CTTGTCTTCCTAAACACCGCAGTCTT
TB5R'	CTGGCTCATTATTGTCCTTGTCTTCC
TB6F'	GGAAGACAAGGACAATAATGAGCCAG
TB6R'	GGAGATGACAAGAAGGAAACAGATGC
TB7F'	GCATCTGTTTCCTTCTTGTTCATCTCC
TB7R'	GGAAGGAGATGACAAGAAGGAAACAG
TB8F'	CTGTTTCCTTCTTGTTCATCTCCTTCC
TB8R'	GAGATGGAAGGAGATGACAAGAAGGA
TB9R'	GAGGAGGATTTGAGAGGTTATCTGGA

The first part of 3' RACE PCR experiment was held with TB4R' on SMARTer Muscle template. In the second part of the 3'RACE PCR experiment (nested RACE PCR), the product of the first RACE PCR were diluted and used as template with TB5R'. The product of nested RACE PCR shown in Figure 4.2 was sequenced by Illumina Miseq Platform.

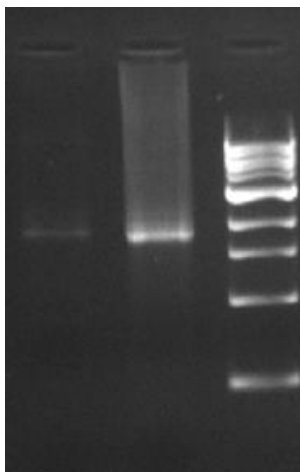


Figure 4.2. Image of Gel electrophoresis: Lane 1: Product of the First RACE PCR with TB5R'. Lane 2: Product of nested RACE PCR with TB4R'. Lane 3: 1kbp Ladder.

The sequence obtained from the *de novo* assembly of 3' RACE PCR product was named as Fragment-1 (Figure 4.8) and was aligned well with *Homerus americanus*' L-type calcium channel sequence in the 5' region. Therefore, primers given in Table 4.4 were designed from Fragment-1 and *Homerus americanus* calcium channel sequence.

Table 4.4. Primers from Fragment-1.

Name of the Primer	Sequence 5'→3'
CaV22L1f	GATTATTCTGGGTGCCTTCTTCGTC
CaV22L2f	GATTCTTGGTGCCTCAGTGGAGAG
CaV22L3f	GAGGAGGATTTGAGAGGTTATCTGG
CaVhaL1r	ATGAACTGGACCAACATCTTCCGTG
CaVhaL2r	TCACAGTGTTGGCAGAGTCTTTGTC

The primers were paired with each other and PCR experiments were done. Successful PCR product was obtained with the pair of CaV22L3f and CaVhaL1r (Figure 4.3).

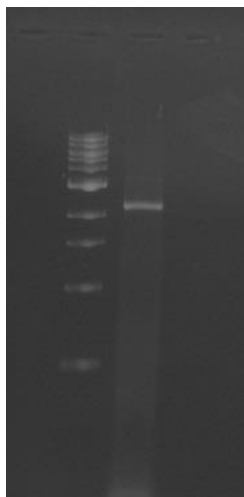


Figure 4.3. Image of Gel electrophoresis: Lane 1: 1 kbp Ladder. Lane 2: The product of PCR with CaV22L3f and CaVhaL1r.

The product was sequenced by Illumina Miseq platform and the resulted sequence of *de novo* assembly in DNASTAR was approximately 2 kbp and was named as Fragment-2 (Figure 4.8). Fragment-2 had overlapping region with Fragment-1 and extended the Fragment-1 to the 3' end. This extension of sequence was approved by aligning with *Homerus americanus* L-type calcium channel sequence. Primers given in Table 4.5 were designed from the sequence of Fragment-2.

Table 4.5. Primers from Fragment-2.

Name of the Primer	Sequence 5'→3'
CaVm31L1f	ATGGATGATGGTGACGATGGACAG
CaVm31L2f	ATTATGGTGATGATGACCTCGGTG
CaVm31L1r	ATGAAGCCATATGACACAACCTTCAGG
CaVm31L2r	TGACATTACTGAAGAGACTGTGGTTGC

Although pairs of the primers in Table 4.5 were successful in PCR experiments, they failed to produce any products in RACE PCR experiments. In order to solve this problem, a different approach was used. The amino acid sequence of Fragment-2 was obtained in MATLAB platform and used in BLAST for Proteins in NCBI. The alignment with maximum score was with amino acid sequence of *Scylla paramamosain's* L-type voltage-gated calcium channel.

In the result of the literature search, four repeat of amino acid motifs given in Table 4.6 related to ion selectivity were found (41). While 1st and 2nd repeat motifs were detected on Fragment-2, 3rd and 4th repeat motifs were found on the sequence of *Scylla paramamosain's* L-type voltage-gated calcium channel and from that sequence's repeat motif regions, degenerate primers given in Table 4.7 were designed.

Table 4.6. Repeat motifs related to ion selectivity.

1 st Repeat Motif	QCITMEGWTDMMY
2 nd Repeat Motif	QILTGEDWNVVMY
3 rd Repeat Motif	TVSTFEGWPGLLY
4 th Repeat Motif	RSATGEAWQEIML

Table 4.7. Degenerate primers from 3rd and 4th repeat motifs of *Scylla paramamosain's* L-type Cav.

Name of the Primers	Sequence 5'→3'
CaVaaR3f1	WSIACNTTYGARGGNTGGGG
CaVaaR3r1	CCCCANCCYGCRAANGTISW
CaVaaR4f1	GCNACNGGNGARGCNTGGCA
CaVaaR4r1	TGCCANGCYTCNCCNGTNGC

The primers were paired with each other for PCR experiments. Successful product from the PCR with the pairs of CaVm31L1f and CaVaaR4r1 was extracted from the gel and sequenced by Illumina Miseq Platform. The obtained sequence after *de novo* assembly in DNASTAR was approximately 1,5 kbp and named as Fragment-3 (Figure 4.8) Fragment-3 had overlapping region with Fragment-2 and extended the Fragment-2 to the 3' end. Fragment-3 was controlled by doing PC experiment with primers CaVm31L1r and CaVMMTf1 (a primer designed from Fragment-3). The result of the control PCR was successful.

In order to reveal further parts of 3' end of the sequence, primers given in Table 4.8 were designed from Fragment-3. Although CaVm31L1f/CaVm31fR4r2,

CaVm31R4f1/CaVm31R4r2 and CaVm31R4f2/CaVm31fR4r3 pairs were successful in PCR experiments, they failed to produce any products in RACE PCR experiments.

Table 4.8. Primers from Fragment-3.

Name of the Primers	Sequence 5'→3'
CaVm31fR4f1	AGCAATTTTCGGTGGTGAAGATCCTC
CaVm31fR4f2	GGCCTTCAGATTCAAGTACTTTGG
CaVm31fR4r1	AAGCACACGGAGGATCTTCACCAC
CaVm31fR4r2	TTCAGCATGATGAGGACAAAGATGG
CaVm31fR4r3	GAACAAACGGAAGAAGTTGATGGAG

In order to improve specificity of the primers we focused onto the voltage sensor sequences, common in most calcium channel sequences (79). These repeat sequences were given in Table 4.9. In addition to voltage sensor sequences GPHH and IQ conserved domains were used for primer design (80).

Table 4.9. Repeat sequences related voltage sensor.

1 st Repeat Motif	KALRAFRVLR
2 nd Repeat Motif	RLLRVFKVTK
3 rd Repeat Motif	VKILRVLR
4 th Repeat Motif	FFRLFRVMRLVKLLS

Primers given in Table 4.10 were designed from the repeat sequences and two conserved domain regions' sequence. The pairs of CaVm31R4f4 and CaVm31R4f5 with CaVspR4r1 were successful in control PCR experiments, CaVm31R4f4 and CaVm31R4f5 were used in nested RACE PCR experiments which had a weak band (Figure 4.4).

Table 4.10. Primers from voltage sensor's repeat motifs and conserved domains.

Name of the Primers	Sequence 5'→3'
CaVmotf2	CTTCTCCGTCTGTTTCGTGTGATG
CaVm31fR4f3	CTCCATCAACTTCTCCGTTTGTTT
CaVm31R4f4	GGGCTCTAACCTCTTCTCCATCAAC

CaVm31R4f5	ACCTCTTCTCCATCAACTTCTTCCG
CaVspR4r1	CATGATCTCCTGCCACGCCTCAC
CaVgphhf1	AAGCACCTTGATGTGGTCACTCTTC
CaVgphhr1	GAGAAGAGTGACCACATCAAGGTGC
CaViqr1	CTGGATGAGGAAGGTTGCGTAGAAC
CaViqr2	GATGTTCTAACCAACGCAAAGAGCG

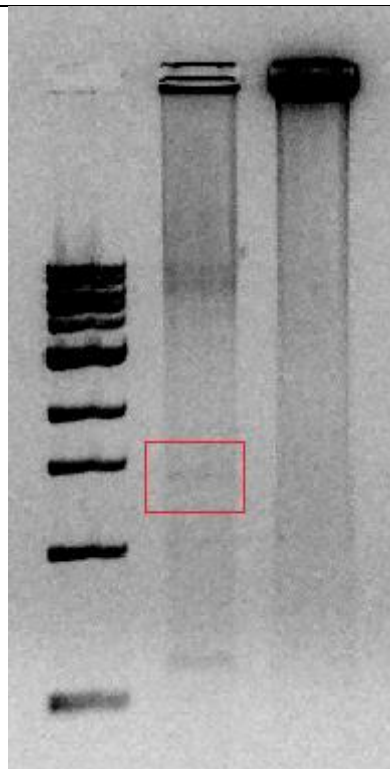


Figure 4.4. Image of Gel electrophoresis: Lane 1: 1 kbp Ladder. Lane 2: The product of RACE PCR with CaVm31R4f4. Lane 3: The product of nested RACE PCR with CaVm31R4f5.

The DNA product in that weak band was extracted from agarose gel and sequenced by Illumina Miseq Platform. The obtained sequence after *de novo* assembly in DNASTAR was approximately 1 kbp and named as Fragment-4 (Figure 4.8). Fragment-4 had overlapping region with Fragment-3 and extended the Fragment-3 to the 3' end. Primers given in Table 4.11 were designed from Fragment-4.

Table 4.11. Primers from Fragment-4.

Name of the Primers	Sequence 5'→3'
CaVMCf1	TAGATCAGCAACAGGTGAGGCATGG
CaVMCf2	TGGACAACCTTTGACTACCTGACACG
CaVMCf3	GCCAGTTGGAGTTGAAGATGATGTC
CaVMCr1	AATGTCATCATCACGCATTTTCATCC

The primers were paired appropriately with each other and their efficiencies were tested. After the test, in nested RACE PCR experiment with CaVMCf1 and CaVMCf2, a successful band was obtained (Figure 4.5).

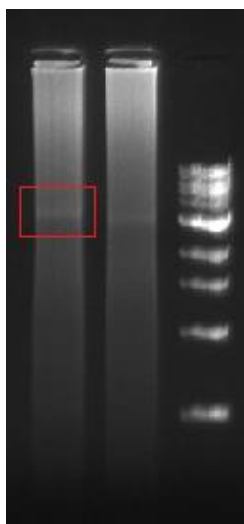


Figure 4.5. Image of Gel electrophoresis: Lane 1: The product of nested RACE PCR with CaVmCf2. Lane 2: The product of nested RACE PCR with CaVmCf3. Lane 3: 1 kbp Ladder. The image in Right: The extraction of the band from the gel.

The product of the band was extracted and sequenced by Illumina Miseq Platform. The obtained sequence after *de novo* assembly in DNASTAR was approximately 2 kbp and named as Fragment-5 (Figure 4.8). Fragment-5 had overlapping region with Fragment-4 and extended the Fragment-4 to the 3' end.

After obtaining Fragment-5, ORF sequence of the voltage-gated Calcium channel's gene was completed in 3' end. This information was confirmed by an analysis in NCBI Blast and Conserved Domains Database. In order to reveal 5' end to complete the full mRNA sequence, primers given in Table 4.12 were designed for final RACE PCR experiments.

Table 4.12. Primers for final RACE PCR experiments.

Name of the Primers	Sequence 5'→3'
CaV5raceR2	TGCCTTCCTCCTCCTCAGCATCTCCAAG
Cav3raceF	AGAGAGTCACGGGACCCATCCAGACAAC

RACE PCR reactions for revealing 5' end was performed with CaV5raceR2 and had a successful band in electrophoresis gel image (Figure 4.6). This band was extracted from the gel and sequenced by Illumina Miseq platform.

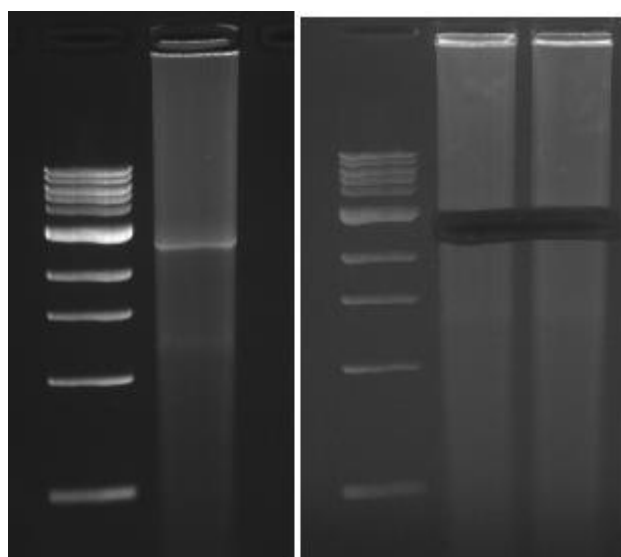


Figure 4.6. Image of Gel electrophoresis: Lane 1: 1 kbp Ladder. Lane 2: The product of RACE PCR with CaV5raceR2. The image in Right: The extraction of the band from the gel.

The obtained transcript from *de novo* assembly, extended the ORF sequence with a “ATG=Methionine” start codon (Figure 4.7). This extension of the ORF was controlled with results of PCR experiments and Sanger Sequencing.

RACE PCR experiment in 3'end was done with CaV3raceF (Figure 4.7). The band of interest was extracted and sequenced by Illumina Miseq Sequence platform.

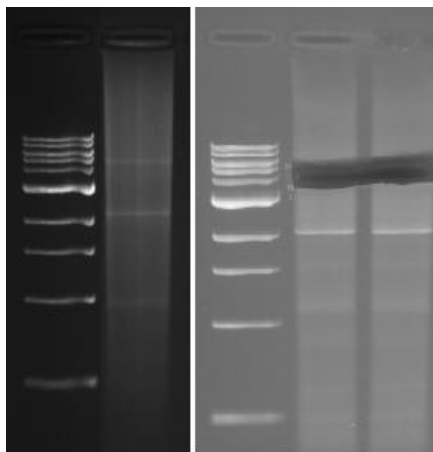


Figure 4.7. Image of Gel electrophoresis: Lane 1: 1 kbp Ladder. Lane 2: The product of RACE PCR with CaV3raceF. The image in Right: The extraction of the band from the gel.

Obtained sequence from RACE PCR experiment for 3' end didn't extend the ORF sequence further, but extended the UTR (UnTranslated Region) sequence in 3' end (Figure 4.8).

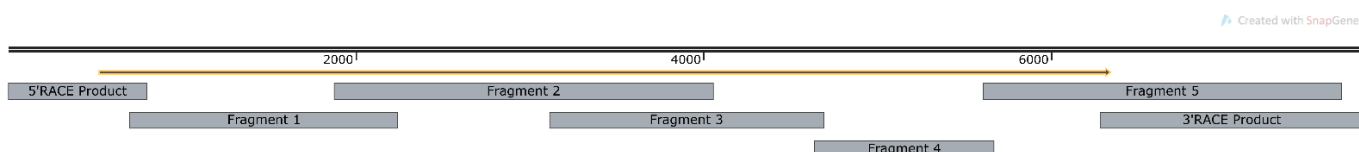


Figure 4.8. Map of the complete sequence (black) with ORF (orange). Alignment of the fragments (grey).

The complete sequence of *Astacus Leptodactylus*' L-type voltage-gated Calcium channel, given in Figure 4.9 the ORF of this gene was shown in bold characters.

```

GGGGTAGTCGTCGTCAGGCGAGTGTGGCTGGCCGGCGAGGCTGAGCTGTCTCCAGCCGCCGAGGGAAGG
AACGGAGAGGGTGGCGGTGGAGAAAGGGTCTGTTGCCGGGTTTTACAGTGAGGTGTGAGCTCAAGGGACGC
GAGTGGTGTCCAACCCGCTCTCAAGGGGCACCCAGGCCTCTAGTTCTGGCCCGCGCCTTGTGATAGGGGAA
TTGGAATCCTTTTGACACCCCTCAATCGCATATCTTAAGGTACAGTGAATCGGTGAATGGAAAGATATAAAGTT
TGTAGAGTGTATGATCCGTGGAGAGAAATATCAGTGAAGCTCATGATAGAGGGATTATTGTGTCCTGTGAA
TACATTTTGTAAAGAAGAAATTCGAGGCGCCGACGCCAAGACGTACAACACCCGGTGACCAAGGAGACGACGC
CGACGCCAAGACGTACAACACCCGGTGACCGAGGAGACGACGCCGACGCCCTAAGACGACCCGGGAGCTTT
AATTCGTACCAAGATGCCTGCGCAAAAATTCCGGGCTCGGATAAAAGGAGCAAAGTATAACCCGGAACA
GACCCAGCAATGAAGGACGAATTCGGCGAATACTCACGAAAGCCGCATCGGAGGAGGAAGAGACCCAAG
TTCAAGACGCGATTAACTATGGGGCGTTCTCAATAGCCCAAGGTCTTTGTGAAGGTGGAGAGGTCCGGGGCG
TCGCTGGGGTACGCTCAGGGGGAGGAGAGAAGCCCTTGTCTGTCGGCGTGGCAGGCAGCACTGAGTGGGG
CCACCTCATGTCTCGCAGGGCCAGGTACCCAACAACGCTACGGACGCTCCCGCGCAGGACGGAAGCGGCC

```

CCCCCGCCGGCCCGTGGGCAAGCCTCCAGAGAACCGGCCAGCTCGTGCACTCTTCTGCCTGGGCCTCAAG
AACCCGCTCAGGAAGGTCTGCATAGACGTGGTAGAATGGAAACCGTTGAGTGGTTTATCTTATTTACCATC
TTCGCCAACTGCGTGGCGTTGGCCGTCTACACGCCCTACCCAACTCAGACTCCAACGCCACAAATGCACAAT
TAGAACAAATTGAGATCATCTTCATGGTGATCTTACTCTTGAGTGCTTTATGAAGATCATAGCATACGGGTT
TGTCTCCATCCAGGAGCTTATAAAGAAGTGTATGGAATACTTTAGATTTCTCATTGTTGTCATAGGGTTG
GTGAGCGGGCATTGGACTTCTTAATGCAAGGGGAGGGAGGGGAGGCAGGGTTCGATGTGAAGGCCCTA
AGAGCCTCAGAGTCTGCGTCCCCTCAGACTTGTCTCTGGTGTCCAAGTCTCCAGGTGGTTTTGAAGTCTAT
TCTGAAGGCTATGGTCCCCTGCTCAACATTGCTCTTCTGTTATGTTTGCATCATCATCTATGCCATCATTG
GTCTGGAGCTTTTCTCCGGTGCCTTCATTTACATGCTATAATAATGAAACAGGGAATCGAATGGAGTCGC
CTCATCCATGTGACAATGGTACAGCAGGTTTTAACTGCTCGGAACCAACAAAGAGGTCAATTTTGGGTGT
GCCGAGATGGCTGGGAAGGACCCAATTATGGCATTACAACTTTGATAATTTTGGCCTCGCAATGCTTACAG
TTTTCCAGTGCATACCCATGGAAGGCTGGACAGATATGATGTATTATATTGCAGATGCCATGGGCAACAGTT
GGCAATGGATCTTCTTTGTTCTATGATTATTCTGGGTGCCTTCTCGTCATGAATCTGATTCTTGGTGTCTC
AGTGGAGAGTTCTCAAAGAGAGAGAAAAGGCACAGGCACGAGGAGACTTCATGAAATTGAGGAAAAAA
CAGCAAATTGAGGAGGATTTGAGAGGTTATCTGGAATGGATAACAGCAGCTGAAGATATTGAGATGGAAG
GAGATGACAAGAAGGAAACAGATGACGGGCGCCGTTTAGTACTGCCGGGAACAAGCAACCGTGGAGCCAT
GTCGGTGGCCTCCCAACTTCCCTTCTGCTCTTCTGCCCTCTTCTCTATGCGTAACTCTAAAGCTGTAGAGAT
TGATGCTGATAAAGGTGATGACAATGATGATGCACAACAGCCGTCATGGTGGCAGAGAAAAGAAAAAAGGA
TTTGACCAATTAATCGGAGAGCGAGGCGGGCGTGTGCAAGGCGGTTAAATCTCAAGCTTTTTACTGGCTC
ATTATTGCTTGTCTTCTAAACACCGCAGTCTTGGCCAGTGAGCACTACCGCCAGCCTGACTGGCTCAGTC
AGTTCCAAGATTATACAAATCTTTCTCGTGGTGTCTTACATGTGAAATGTTGTTAAAAATGTACAGTTT
AGGCTTCAAAGGCTACTTTGTATCACTGTTCAACCGTTTTGATTGCTTTGTGGTTATCAGTAGTATCACTGAG
GTGGTACTCACCTTACCAGAAATAATGCCGCCCTTGGAGTCTCTGTGCTCCGTTGTGTCAGGCTTCTCAGAG
TCTTCAAAGTTACAAAATACTGGCGGTCGCTCTCAACCTGGTTGCTTCCCTCCTCAACTCCATCCAGTCGATC
GCCTCTTGTGCTCCTGCTCTTCTTATTATTATCTTGTCTCCTGGGCATGCAAGTCTTCGGTGGCCGC
TTTAATTTAATCCGACTGAAGATAAACACGTCATAACTTTGACAACCTTCGTTACAGCCATGTTGACAGTGT
TCCAGATCTTGACGGGTGAGGACTGGAACGTTGTGATGTATGATGGAATTCGTGCCTATGGTGGAGTAGCA
ACTCCTGGCATCATTGCCTGTGTCTACTTCATCATTCTTTTCTGTGGTAACTATATCTTGTCTCAATGTCTTC
TTGGCCATTGCTGTGGATAACCTGGCTGATGCAGATGCACTTGGAGATGCTGAGGAGGAGGAAGGCCAAAG
AAGGGGAAGAGGGTAGAGAAGGAGATGGGGGTGAAGGAGAGAGAGAGAAAATTTAAATGGAAGGGGA
AGATGGCTTAGAAGCAGAGGAAAAGACTGCATTGAATCATATAGCTTTAAGAGACGGAGAGACAGCAAGT
CATACCAAAGTACATCTAGGGATGGATGATGGTGACGATGGACAGAAATATGATGATGATGATTATGGTG
ATGATGACCTCGGTGAAGAAGAAGAGGATGATGGTGTGAGAGGAGCGCCACAAGGAATGCGGCCAC
GCCGTGCCTCGCAACTTAGTACTGCCAACAAAGTCAAGCCTTTGCCCCGTACTCCAGCTTTTTTATTTCTCC
CACACAAACAGGTTCCGTGTTTTCTGCCATACTGTGTGCAACCACAGTCTTCTCAGTAATGTCATTCTTGTCTG
CATTCTCATCTCATCTGGCATGTTGGCTGCTGAGGATCCTCTTCTGCTGACTCTCAACGCAATACTATCTTGA
ACTACTTTGACATCTTCTTACATCAGTGTTTACAGTTGAAATCTTCTGAAAGTTGTGTCATATGGCTTCATC
TTGCATAAAGGCGCCTTCTTCTGTTCTGCCTCAACGGCTTAGATCTGTTGGTTGTGGCCGTTTCTCTCATCTC
ATTTCTTTCAAGGATGGAGCAATTTCCGGTGGTGAAGATCCTCCGTGTGCTTCGTGCTCAGGCCTCTCCGT
GCAATCAACAGGGCAAAGGGCCTCAAGCATGTAGTTCAGTGCGTCATAGTGGCTATCAAGACCATCGGCAA
CATCATGCTGGTTACCTGCCTTCTTGAAGTTCATGTTGAGTAATCGGAGTTCAGTGTTCAGGGCAAGTTC
TTCCGTGTAACGACAGGTCCAAAATCTTGGAGTCAAGATTGTAGGGGTCAATTTATTGTCTACCATGATGGA
GATATTACCAAGCCTATGGTGGAGAAGAGAGTCTGGGAGAAAAATGCCTTTCATTCGACAATGTAGCCAA
AGCTATGTTGACGCTTTCACAGTGTCTACATTTGAGGGCTGGCCTGGGTTGTTATATGTGTCATCGACTCC
AACACTGAAGATGTTGGTCTGTGCACAACCTACCGCCCTATGGTAGCCGCTACTACATCATTACATCATCA
TCATTGCCCTTCTCATGGTTAACATCTTCTGTTGGTTTTGTTATCGTCACATTCCAGAGCGAGGGTGAACAAGA
GTACAAGAATTGTTGCCTGGATAAAAATCAGAGAACTGCATAGAATTTGCTCTGAAAGCCAAACCGGTTA
GACGCTATATTTCCAAAACCGGTTTCAATACAAAATATGGTGGTTTGTACCTCACAACCTTTGAATACGC
CATCTTTGCTCTCATGCTGAACACTGTCTTTGGCAATGAAGTTTCGAGGAGAACCAGAGATATACACT
CATGCCCTTGACATTCTCAACCTCATCTTACGGCTGTCTTTGCTCTTGAATTTGTTCTCAAGATAATGGCCTTC
AGATTCAGTATTACTTTGGCGATGCCTGGAATGTGTTTGTATTCGTCATTGTCCTTGGCAGCTTCATTGATA
TCGTCTATTAGAAAGTCAATCCGGGCTCAACCTCTTCCATCAACTTCTTCCGTTTGTCCGTGTGATGCGTT
TGGTGAAGCTTCTCTCAAAGGTGAAGGTATCCGGACGCTACTGTGGACGTTTCATCAAGAGTTTCCAGGCTC
TGCCCTACGTTGCTCTTCTCATCCTCCTCTTCTTCTCATCTACGGCGTGGTGGCATGCAGGTTTTTGGCAAGA
TTGCATTTGACTACACAACACAGATTCATCGTCATAACAATTTTCCAGACCTTCTTCAAAGCAGTAATGGTTCTC

```

TTTAGATCAGCAACAGGTGAGGCATGGCAAGAAATCATGTTGTCGTGTTACCACCGGATGCTGGCTGTGAT
CCCCAGTCTGAAGACTACCCAATGCTCGCACCTGTGGCTCAATGGTTGCATATCCTTACTTCATATCCTTCTA
CACCTATGTTCACTTCTTGATCATCAACTTGTTTGTGCTGTCATCATGGACAACCTTGACTACCTGACACGGG
ATTGGTCTATCCTTGGCCACATCATCTGGATGAGTTCATCACACTGTGGTCAGAGTATGACCCTGATGCTAA
GGCAGAATTAACATTTAGATGTGGTACTCTTCTCAGGAAAATATCTCCCCATTGGGATTTGGAAAATT
GTGCCCATATCGTGTAGCGTGTAACGTTTGTAGTGGCAATGAATATGCCTTTAAATACAGATGGAACAGTGAT
GTTCAATGCAACACTTTTTGCCTTAGTTAGAATCCTTAAGAATAAAAACAGAGGGCAACATTGATGATGC
CAATGAAGAGTTGAGAGCTGTCATTAAGAAGATCTGGAAGCGTACAAATCTAAACTTCTGGATCAAGTTG
TTCCGCCAGTTGGAGTTGAAGATGATGTCACTGTGGGCAAGTTTTATGCCACTTTTCTAATCCAAGATTACTT
CAGAAGATTTAAAAAGAAGAAGCAAGAAATTAAGAACAAATTGATAAAGACTCTGCTAACACAGTCACA
CTGCAGGCTGGTTTGAGAACTTTGCATGAAGCAGGCCCGAGCTGAAGCGCGCCATCTCGGGCAATCTGGA
TGAAATGCGTGATGATGACATTCCACGCATAGGATGGGTAATATCTGCATCTGTTATTCTCAAGGTCAA
CAACCAGATTATGAATATGATATCTCTACAAACTCACTCTCCTACTCTCCTGCACATTCTAATGAGAAGACT
GCATTAATCACACAGCACATCGGCCCTCTACTCTTGAAGCTCTCAATCTCTGGGTGAGGACGATGAA
GGGATCCAATGCGCCCACTTAGGATAATGAACGGGGATCCTGAAAGAAGATCTAATCTAGTAATAAAGA
CAAACAAATGCAGTATTTGACGCCAGATTATCATGCGACCTCTCTCAGTGAGAGTAATGGAAGCCTTCCAGG
GGACCGCCACTCCCAAAGTGTCCCGAGCAGTCCAGAAGTGTGTCCAGACCTTATTCTGAGGTTGTGGGCTC
CGCCGAGAGTTTGGTCCGCAGGGTGTGGCTGATCAGGGTTTGGGGAAATACTGTGATCCTGAATTTGTAC
GTACAACCTCAAGGAAAATTGCAGAGGCCTTGGAAATGACCACAGAGGAAATGGACCGAGCTGCTCACAA
TATTCTCTGCTTCCCAACAAGAAGTCCCTGAGGATGTCTCTTGTAGCATTCCCAACGACAAAGAGAG
TCACGGGACCCATCCAGACAACAAAAACAAGATTCATCATATTATGATCACCATCACCTTATAGAAATAC
GTAAATTAGAAACCTTCTAATTCTGTTATATGGTGGATCATCAATGTGTCCATTCACTCTTCCAACCTCATGA
TTCGTATGTGTCTATTGGAGGCTTTGTGAAGAGGCCTTCTGAAGATGCTCGTACAAGGGTTATTAAGTGCTCT
GGAAAGAGAACCCACTTTGGTCTATGGTCTGCCCTCAAGCTGCCTCTGCTCTGTGGATGTTCTTCTATGG
GAGACAGAGAGGGATAACAAAAATAAGATTTTCTAGGGCATCTGTTGAAGGTGGAAGGACAGGATGAGGTA
GTGCTATTCTCCAACTTGTGAATAATTTATACTTGTGAGTATAGTCACGTTCTCATCTTGAAGGGAATCAC
AAGAGTTTGAACCTACACTATTCTATAATGCTGATGAACTGCATCAGGAAGTATGGCAAAGCCTATTTTTT
ACATACAGCTGTTTATGTGGTAGGGTGAACGAGTCATATTTGTTAGGATCTCGTTGTTTGGTTTGTGTACAAGC
AATTGTTGGTTCACCCAGTGTGGTGAAGTACCCACAGAAGGCTTATCCCTGTGTGTGGGTTCTCCTTAACAA
AGGGATTGAGGTATGTGAAATGATGAGCAGATTCTAGTTCCGAGATGCTTTCAGTAAGATTATTTTTGTAAT
GTAAAATGAAATCTTACAGGAAGTCTGCTCCAGTTATTAGACAGCATATCTTTCATATATCTTTATCTTTGAGCT
CGCACTTGGAAAGTTATCATATCCCTGAATTTCTGGGGATATTAAGCAAATGTTATGTCAATTCTCTAAGGTT
AGGTAATTACCTAAGTGAATTACCTAAGTGAATTACCTAATTAATTATCTAAGGTGTAAGACAAGTATTGTA
TTCCCTGAATGAGGGTCAAGGCAGATTGTCTACCGTATTCCTTACCAGTAATGGGACGTAGCACTATGCGCAG
ATCATATCTCCATTATCCTCAGGCTATGAGAACCAGCAAGTGAATCAATGCTGTATAACCTCTACACATTTG
AGTAGGGGTTAACTTATTTAACCCAAAGTGCCTCTCTCAATTGTGATAATCTGTTGTTATTTCTCTCAAACAAG
TTTCATTGAAAGGTAAGTAAATCACCTCATGTCATCCATAATTTCTTGCAGTTTCTGTCTCTTAGGAATTTGCTTG
TTTTCTTCCAGAGTTCAATTTGATGGTCATTATCATTATTATTAATATTCTATTGTTTTTATTAATTTTTTATTTT
TGCTTGACCAGAAAAGCTGGCAGGCGGCTCACACTTTTTTTTTTTTTTTTTTTTTTTTTTTGGGGGGGGGGGGGG
GGGTGGGGGGGTTTTTTTTTTTTTTTGGGAGGGGAGGCAGAATACCCACGTTTTTTAATAAACATTTCCGGGCC
AAAGAAACGGGAGCAAATACCGATTG

```

Figure 4.9. The complete sequence of L-type voltage-gated Calcium Channel.

GPHH and IQ domains, the segments of ion selectivity, domains of voltage sensor and the DHP binding sites were marked on the complete sequence of cloned mRNA (Figure 4.10).

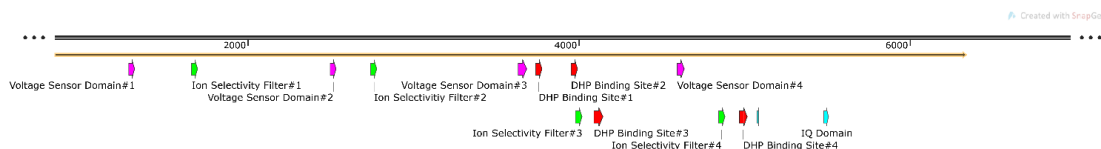


Figure 4.10. Map Image of complete sequence and fragments of voltage sensor, ion selectivity filter, DHP binding sites, IQ and GPHH domain.

The complete mRNA sequence was translated to the amino acid sequence. The calculated protein sequence was submitted to NCBI Blast platform. It was observed that the sequence had high percentage coverage and high score alignments with the sequence of voltage-gated calcium channels in closely related species (Figure 4.11).

Description	Scientific Name	Max Score	Total Score	Query Cover	E value	Per. Ident	Acc. Len	Accession
<input checked="" type="checkbox"/> voltage-gated calcium channel [Astacus leptodactylus]	Astacus leptodactylus	4029	4029	100%	0.0	100.00%	1942	WCO13213.1
<input checked="" type="checkbox"/> muscle calcium channel subunit alpha-1-like isoform X28 [Eriocheir sinensis]	Eriocheir sinensis	3296	3296	100%	0.0	86.07%	2031	XP_050688137.1
<input checked="" type="checkbox"/> muscle calcium channel subunit alpha-1-like [Homarus americanus]	Homarus americanus	3287	3287	96%	0.0	86.28%	2037	XP_042203788.1
<input checked="" type="checkbox"/> muscle calcium channel subunit alpha-1-like isoform X28 [Penaeus japonicus]	Penaeus japonicus	3228	3228	100%	0.0	83.31%	2045	XP_042859893.1
<input checked="" type="checkbox"/> muscle calcium channel subunit alpha-1-like isoform X29 [Penaeus japonicus]	Penaeus japonicus	3219	3219	100%	0.0	83.07%	2045	XP_042859894.1
<input checked="" type="checkbox"/> muscle calcium channel subunit alpha-1-like isoform X31 [Eriocheir sinensis]	Eriocheir sinensis	3214	3214	100%	0.0	84.51%	1998	XP_050686144.1
<input checked="" type="checkbox"/> muscle calcium channel subunit alpha-1-like isoform X25 [Penaeus japonicus]	Penaeus japonicus	3212	3212	100%	0.0	82.07%	2075	XP_042859890.1
<input checked="" type="checkbox"/> muscle calcium channel subunit alpha-1-like isoform X26 [Penaeus japonicus]	Penaeus japonicus	3208	3208	100%	0.0	82.11%	2074	XP_042859891.1
<input checked="" type="checkbox"/> muscle calcium channel subunit alpha-1-like isoform X24 [Penaeus japonicus]	Penaeus japonicus	3202	3202	100%	0.0	81.87%	2075	XP_042859889.1
<input checked="" type="checkbox"/> muscle calcium channel subunit alpha-1-like isoform X30 [Penaeus japonicus]	Penaeus japonicus	3198	3198	100%	0.0	82.53%	2045	XP_042859895.1
<input checked="" type="checkbox"/> muscle calcium channel subunit alpha-1-like isoform X22 [Penaeus japonicus]	Penaeus japonicus	3195	3195	100%	0.0	81.56%	2083	XP_042859887.1
<input checked="" type="checkbox"/> muscle calcium channel subunit alpha-1-like isoform X23 [Penaeus japonicus]	Penaeus japonicus	3192	3192	100%	0.0	81.59%	2081	XP_042859888.1
<input checked="" type="checkbox"/> muscle calcium channel subunit alpha-1-like isoform X36 [Portunus trituberculatus]	Portunus trituberculatus	3174	3174	98%	0.0	84.95%	2089	XP_045108544.1
<input checked="" type="checkbox"/> muscle calcium channel subunit alpha-1-like isoform X31 [Portunus trituberculatus]	Portunus trituberculatus	3163	3163	100%	0.0	81.22%	2110	XP_045108536.1
<input checked="" type="checkbox"/> muscle calcium channel subunit alpha-1-like isoform X22 [Eriocheir sinensis]	Eriocheir sinensis	3155	3347	99%	0.0	88.76%	2067	XP_050686129.1
<input checked="" type="checkbox"/> muscle calcium channel subunit alpha-1-like isoform X16 [Portunus trituberculatus]	Portunus trituberculatus	3150	3150	98%	0.0	81.88%	2155	XP_045108520.1
<input checked="" type="checkbox"/> muscle calcium channel subunit alpha-1-like isoform X8 [Eriocheir sinensis]	Eriocheir sinensis	3143	3335	99%	0.0	87.36%	2097	XP_050686113.1
<input checked="" type="checkbox"/> muscle calcium channel subunit alpha-1-like isoform X15 [Portunus trituberculatus]	Portunus trituberculatus	3139	3139	98%	0.0	81.64%	2155	XP_045108519.1
<input checked="" type="checkbox"/> muscle calcium channel subunit alpha-1-like isoform X23 [Eriocheir sinensis]	Eriocheir sinensis	3135	3327	99%	0.0	88.17%	2067	XP_050686130.1
<input checked="" type="checkbox"/> muscle calcium channel subunit alpha-1-like isoform X8 [Portunus trituberculatus]	Portunus trituberculatus	3135	3135	98%	0.0	81.40%	2160	XP_045108512.1
<input checked="" type="checkbox"/> muscle calcium channel subunit alpha-1-like isoform X10 [Portunus trituberculatus]	Portunus trituberculatus	3135	3135	98%	0.0	81.55%	2159	XP_045108514.1

Figure 4.11. The results of the analysis done in NCBI Blast with the gene's protein sequence.

When the amino acid sequence was examined on NCBI Conserved Domain Database, all the domains for ion transport, GPHH, IQ and C-terminal were observed in the sequence (Figure 4.12).



Figure 4.12. The results from NCBI Conserved Domain Database Analysis with the gene's amino acid sequence.

In order to produce the complete sequence of the gene, primers given in the Table 4.13 were designed in MATLAB platform. In result of the PCR experiments with the pair of primers, a successful single band was obtained Figure 4.13. The PCR product was purified and sequenced by Illumina Miseq platform.

Table 4.13. Primers for obtaining complete sequence of the gene.

Name of the Primers	Sequence 5'→3'
cavFk1	TACAGTGAATCGGTGAATGGAAAG
cavRk1	TTTGGGAGAATAGCACTACCTCAT

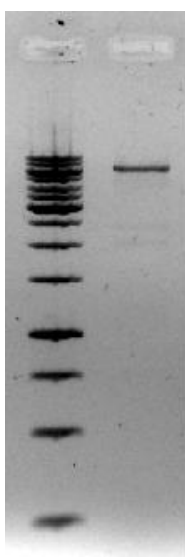


Figure 4.13. Image of Gel electrophoresis: Lane 1: 1 kbp Ladder. Lane 2: The product of PCR with cavFk1 and cavRk1.

To control the relevancy of the cloned mRNA short reads were aligned onto reference sequence at a 93 % similarity constrain. Homogeneous and continuous alignment of the short reads on reference sequence indicated a successful cloning of the target mRNA (Figure 4.14). The complete sequence was submitted to NCBI nucleotide database and accepted with accession code **ON661560.1**.

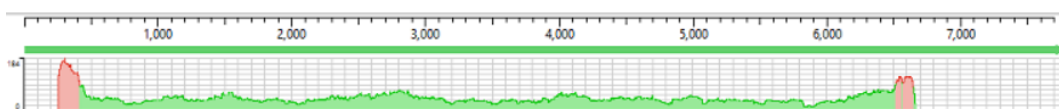


Figure 4.14. Successful alignments of short reads with sequence of the gene.

Our model animal is in invertebrate's division with related species. Phylogenetic tree analysis was done in MATLAB (Figure 4.15). The phylogenetic tree shows that similarity of the cloned sequence was highest in neighboring species. As you can see the first diversion is between vertebrates and invertebrates. After that vertebrates divided into mammals and other.

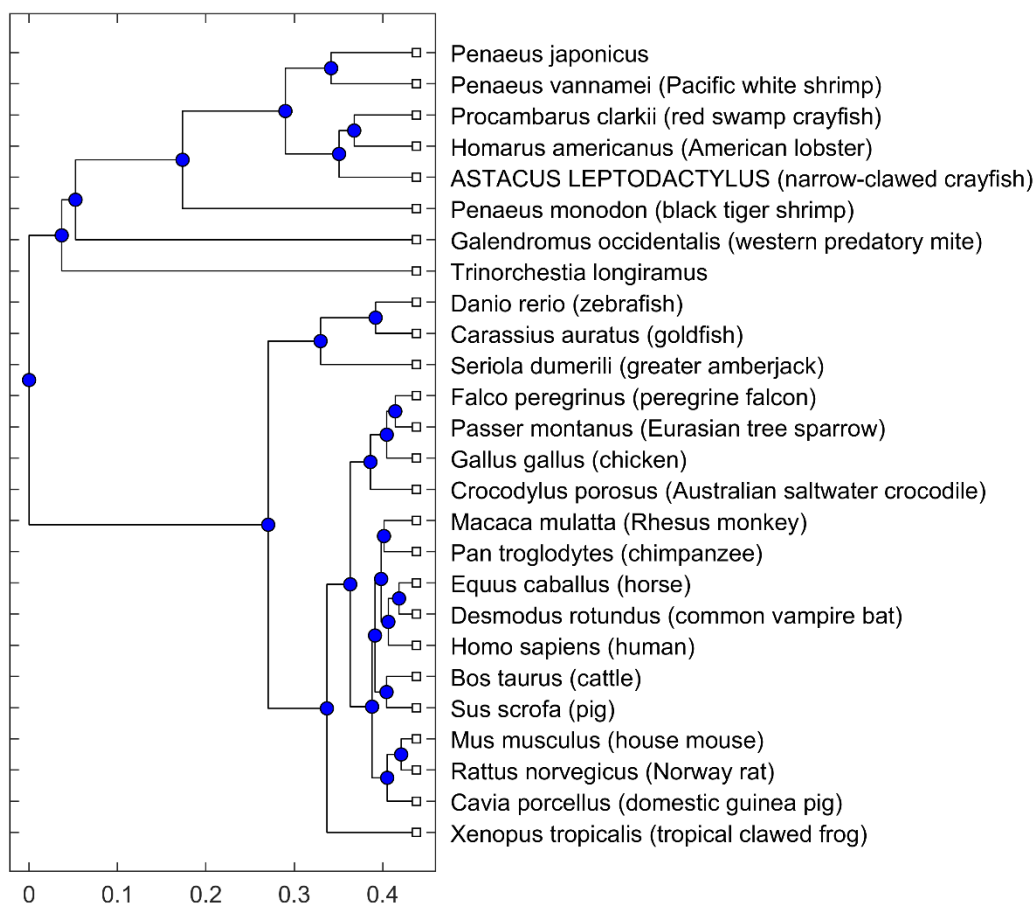


Figure 4.15. The phylogenetic tree analysis for cloned channel.

3D Structure models of the L-type voltage-gated calcium channel was made in Swiss-Model Online platform (82) with the amino acid sequence from translation of complete ORF sequence. Human L-type voltage-gated calcium channel Cav1.3 (7uhg: Electron Microscopy) was chosen as a reference template which generated the best fit and the most accurate three-dimensional structure of the cloned protein (Figure 4.16). The similarity between the amino acid sequence and reference template was 64,76 %.

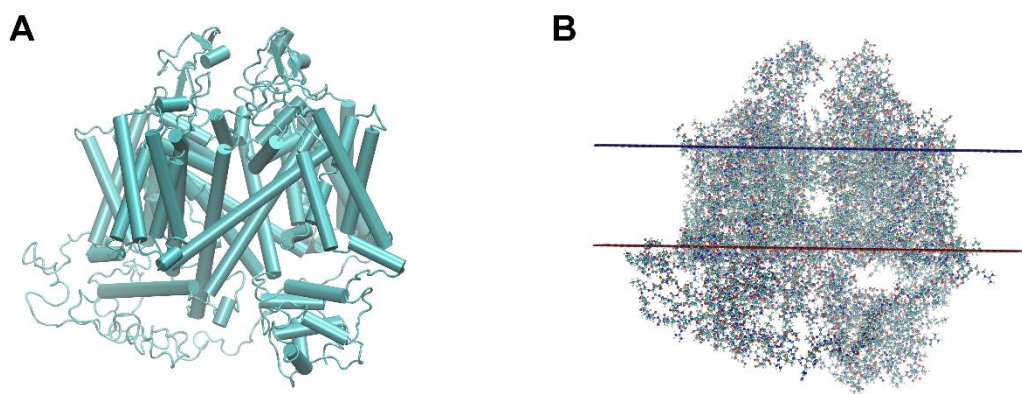


Figure 4.16. 3D Structures of the cloned channel by Swiss-Model. A: 3D structure of channel in VMD'S cartoon mode (83). B: 3D structure of the protein in membrane by MEMEBED Predicition, PSIPRED, UCL (84).

Segments for voltage sensor, ion selectivity filter and DHP binding sites were marked on three-dimensional structure by using VMD (83) and shown in Figure 4.17. It was observed that the selectivity filter consisted of 4 symmetrical domains in the narrowing region of the channel's hole, while the segments of the voltage sensor were close to the outer surface of the channel. It was observed that DHP binding sites had a separate position other than the selectivity filter.

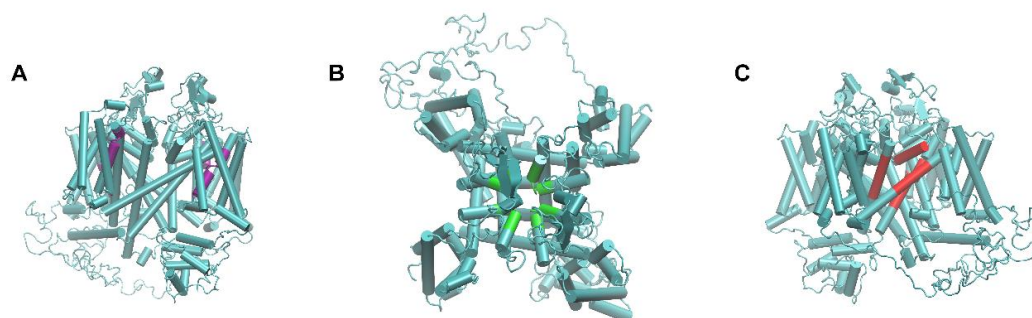


Figure 4.17. Voltage sensor (purple), selectivity filter (green) and DHP receptor (red) regions are shown in A, B and C, respectively.

In order to analyze the interactions between ligand and the channel, docking experiments were performed with blockers diltiazem, nifedipine and verapamil. The results of these docking experiments are shown in Figure 4.18. Diltiazem and verapamil bound to the selectivity filter, but nifedipine, which is DHP, bound to the DHP binding sites.

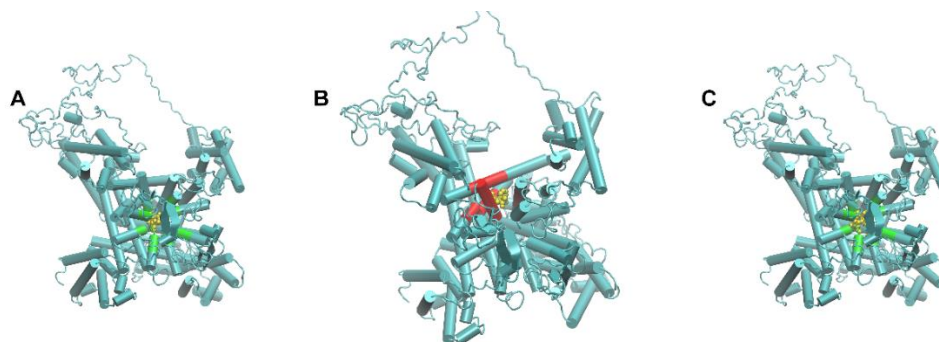


Figure 4.18. Docking of diltiazem, nifedipine and verapamil molecules (yellow) to the cloned channel protein, A, B and C respectively. Green and red segments are the selectivity filters and DHP binding sites, respectively.

In order to assess the functional properties of the calcium channel coded by the mRNA a reference plasmid (a1lc-HE3-pcDNA3) was used. Plasmids were amplified in *E. coli* clones. Amplified plasmids were filtered by using the HiSpeed Plasmid Maxi Kit. Linearized plasmid was used for cRNA synthesis. Two or three days following the injection of cRNA, oocytes were examined by double electrode voltage clamping. As shown in Figure 4.19, a distinct inwardly directed current component was observed in the transfected oocytes. The current component was voltage dependent and activated at a faster rate as the cell depolarized. Loading of EGTA into the oocytes induced a shift in the current voltage relationship where current equals zero (i.e. E_{Ca} becomes more positive).

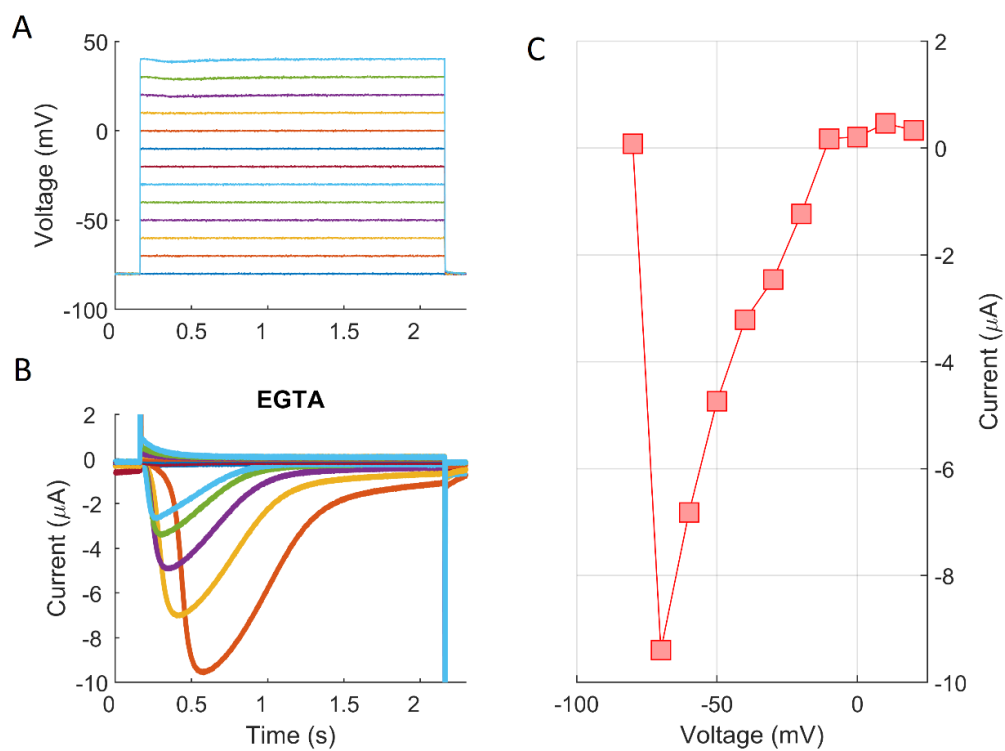


Figure 4.19. Calcium currents from calcium channel plasmid (a1Ic-HE3-pcDNA3) injected oocytes. A: voltage clamp steps. B: Evoked current responses. C: current-voltage relationship.

5. DISCUSSION

Several conserved and functional domains were identified when the ORF region of the cloned mRNA was translated into amino acid sequence (Figure 5.1).

```

MPAQKFRARIKGAKYNPETDPAMKDEFGEYFTKAASEEEETQVQDAINYGAFSIAQGLCEGGEV GASLGSASGGG
EKPLSSAWQAALSGATSMSQGQVPNNATDAPAHKRPPRRPVGKPPENRPARALFCLGLKNPLRKVICDVVE
WKPFWEFILFTIFANCVLAVYTPYNSDSNATNAQLEQIEIFMVIFTECFMKIAYGFVLHPGAYIRSVWNTLDFLI
VVIGLVSGALDFLMQEGEGEAGFDV KALRAFRVLRPLRLVSGVPSLQVVLNSILKAMVPLLNIALLVMFVIIYAIIGLE
LFIGALHFTCYNNETGNRMESPHPCDNGTAGFNCSELNKEGQFWVCRDGEWGPNYGITNFDNFGLAMLTVF QC
ITMEGWTDMMYYIADAMGNSWQWIFFVSMIILGAFFVMNLILGVLSGEFSKEREKAQARGDFMKLKQKQIEED
LRGYLEWITAEDIEMEGDDKKTDDGRRLVLPGTSNRGAMSVASPTSLLLFLPLFSMRNSKAVEIDADKGDNDND
AQQPSWWQRKKKGFDRINRRARRACRKA VKSQAFYWLIVLVFLNTAVLASEHYRQPDWLSQFQDYTNLFFVVLV
TCEMLLKMYSLGFQGYFVSLFNRFDCFVVISSITEVVLSTEIMPPLGVSVL RCVRLLRVFKVTKYWRSLSNLVASLLN
SIQSIASLLLLLFLFIIFALLGMQVFGGRFNFNPTEDKPRHNFDFVQAMLTVF QILTGEDWNVVMYDGIRAYGGV
ATPGIACVYFIILFICGN YILLNVFLAIAVDNLADADALGDAEEEEGKEGEEGREGDGGEGEREKIKMEGEDGLEAEE
KTALNHIALRDGETASHTKVHLGMDDGDDGQKYDDDDYGGDDDLGEEEDDGDGEERPQGMRRPRASQLSTAN
KVKPLPPYSSFFIFSHTRFRVFCHTVCNHSLSFNVLVLCILISSGMLAAEDPLRSDSQRNTILNYDFIFTSVFTVEIFLK
VVSYGFILHKGAFLRSAFNGLDLLVAVSLISFSFKDGAISV VKILRVLRVLRPLRAINRAKGLKHVVQCVIVA IGNI
MLVTCLEFMFAVIGVQLFKGKFFRCNDRSKILESDCRGQFIVYHDGDITKPMVEKRVWEKNAFHFDN VAKAMLT
FTVSTFEGWPGLLYVSIDSNTEVDVGPVHNYPMAVY IIYIIIIIAFFMVNIFVGFVIIVTFQSEGEQEYKNCCLDKNQR
NCIEFALKAKPVRRYIPKNRFQYKIWWFVTSQPF EY AIFVLIMLNTVSLAMKFRGEPEIYTHALDILNLIPTAVFALEFV
LKIMAFRFKYFGDAWNVDFVIVLGSFIDIVYSEVNPGSNLSIN FFRLFRVMRLVKLLSKGEGIRLLWTFIKSFQAL
PYVALLILLFFIYGVVGMQVFGKIAFDYTTQIHRHNNFQTFQAVMVL RSATGEAWQEIMSCLPPDAGCDPQS
EDYPNARTCGSMVAY YFISFYTLCSFLIINLFVAVIMDNFDYLTRDWSIL GPHHLDEFITLWSEYDPAKGRIKHLDV
VTLLRKISPPLFGFKLCPYRVACKRLVAMNMP LNTDGTVMFNATL FALVRTSLRIKTEGNIDDANEELRAVIKIKWK
RTNPKLLDQVVPVGVEDDVTVGKFYATFL IQDYFRRFKKKKQEIKEQIDKDSANTVTLQAGRLTLHEAGPELKRAIS
GNLDEMRRDDIPTHRMGNILHPVILKVNNQIMNMISPTNSLSYSPAHSNEKTALNHTAHRPPTPLESSQSLGEDDE
GIPMRPLRIMNGDPERRSNLVIKDKQMQLTPDYHATSLSSENGSLPGDRHSQSVSPSSPRSVSRPYSEVVGSAESLV
GRVLADQGLGKYCDPEFVRTTSREIAEALEMTEEMDRAAHNLSASQQELAPEDVSLEHSQRQRESRDP SRQQK
QDSSYYDHQSPL

```

Figure 5.1. The Amino Acid Sequence of cloned voltage-gated Calcium Channel. Voltage sensors highlighted in purple, selectivity filter in green, IQ and GPHH domains in blue and DHP receptor sites colored in red.

In human and rabbit L-type voltage-gated calcium channel sequences, ion selectivity domain motifs were found in P-loop_i, P-loop_{ii}, P-loop_{iii}, and P-loop_{iv} [40,

44, 85] (Table 5.1). After the alignment analysis, the ion selectivity motifs in *Astacus Leptodactylus* were identified as shown in Table 5.1. It is important to emphasize that four glutamate residues, essential for calcium selective filter, are present in the cloned sequence (Table 5.1).

Table 5.1. Ion selectivity domain motifs.

Ion selectivity domain motifs in L-type Ca_v of human and rabbit	Ion selectivity domain motifs in <i>Astacus Leptodactylus</i> ' L-type Ca_v
P-loop _i : QCITMEGWTDVLW	QCITMEGWTDMMY
P-loop _{ii} : QVLTGEDWNSVMY	QILTGEDWNVVMY
P-loop _{iii} : TVSTFEGWPQLLY	TVSTFEGWPGLLY
P-loop _{iv} : RCATTGEAWQEILL	RSATGEAWQEIML

In human and rabbit L-type voltage-gated calcium channel sequences, were defined domains of voltage sensor motifs in S4_i, S4_{ii}, S4_{iii} and S4_{iv} [40, 48, 85] (Table 5.2). When the alignment analysis was done with these motifs, the ion selectivity motifs in *Astacus Leptodactylus* were identified as shown in Table 5.2. The polar amino acid residues are necessary for voltage sensing. Thus, the cloned putative calcium channel protein possesses four segments, as one in each domain, rich in Lysine (K) and Arginine (R) residues (Table 5.2).

Table 5.2. Voltage sensor domain motifs.

Voltage Sensor domain motifs in L-type Ca_v of human and rabbit	Voltage Sensor domain motifs in <i>Astacus Leptodactylus</i> ' L-type Ca_v
S4 _i : KALRAFRVLRPLR	KALRAFRVLRPLR
S4 _{ii} : RCIRLLRLFKITK	RCVRLLRVFKVTK
S4 _{iii} : VKILRVLRVLRPLRAINR	VKILRVLRVLRPLRAINR
S4 _{iv} : FFRLFRVMRLIKLLSR	FFRLFRVMRLVKLLSK

In human and rabbit L-type voltage-gated calcium channel sequences, DHP binding sites sequences were found in S5_{iii}, P1_{iii}, S6_{iii} and S6_{iv} [64, 85] (Table 5.3). Alignment analysis with these sites indicated that similar binding sites are present in the cloned sequence (Table 5.3). As compared to the other binding sites identified

for diltiazem and verapamil DHP binding sites are not homogenously distributed between the domains of the cloned calcium channel.

Table 5.3. DHP binding sites.

DHP Binding sites in L-type Ca _v of human and rabbit	DHP Binding sites in <i>Astacus Leptodactylus</i> ' L-type Ca _v
S5 _{III} : IGNIVLVTTLLQFM	IGNIMLVTCLEFM
P1 _{III} : VLSAMMLFTVST	VAKAMTLFTVST
S6 _{III} : IYYIILIAFFMMNIFVGFV	IYYIIIIAFFMVNIFVGFV
S6 _{IV} : YFISFYMLLCAFLIINL	YFISFYTLCSFLIINL

The relevancy of the identified binding sites has been confirmed by the docking experiments. As shown in Figure 4.17_B the docking experiments identified a binding site for the dihydropyridine similar to that estimated in the alignment experiments [64] (Figure 5.1). The binding site for DHP was clearly different than the selectivity filter of the channel. However, both verapamil and diltiazem docked directly onto the selectivity filter which is in an agreement with the former reports [64]. Structural calculations indicated a successful fit to the reference structure. Four domains and the individual transmembrane segments could distinctly be identified.

The functional experiments indicated that an inwardly carried calcium component was restored in the plasmid injected oocytes. However, a1lc-HE3-pcDNA3 is a human calcium channel plasmid. Thus, it has to be considered on for comparison purposes. Our efforts to synthesis a functional plasmid for the cloned channel failed due to unknown problems.

6. CONCLUSION

In the present thesis work a novel mRNA was *de novo* cloned in the crayfish. Considering the similarity assay in the NCBI platform, the three-dimensional structural calculations and the docking experiments it was concluded that the mRNA codes an alpha peptide for a putative voltage-gated calcium channel protein in the crayfish.

7. REFERENCES

1. Catterall, W. A. Voltage-gated calcium channels. *Cold Spring Harbor perspectives in biology*. 2011; 3(8) a003947. doi:10.1101/cshperspect.a003947.
2. Swerup, C., Purali, N. And Rydqvist, B. Block of receptor response in the stretch receptor neuron of the crayfish by gadolinium. *Acta Physiologica Scandinavica*. 1991; 143: 21-26. <https://doi.org/10.1111/j.1748-1716.1991.tb09197.x>
3. Purali, N., Rydqvist, B. Block of potassium outward currents in the crayfish stretch receptor neurons by 4-aminopyridine, tetraethylammonium chloride and some other chemical substances. *Acta Physiologica Scandinavica*. 1992; 146: 67-77. <https://doi.org/10.1111/j.1748-1716.1992.tb09394.x>
4. Purali, N., Rydqvist, B. Action Potential and Sodium Current in the Slowly and Rapidly Adapting Stretch Receptor Neurons of the Crayfish (*Astacus astacus*). *Journal of Neurophysiology*. 1998; 80: 2121-2132. <https://doi.org/10.1152/jn.1998.80.4.2121>.
5. Purali, N. Structure and function relationship in the abdominal stretch receptor organs of the crayfish. *J. Comp. Neurol*. 2005; 488: 369-383. <https://doi.org/10.1002/cne.20590>.
6. Purali, N. Antidromic potential spread modulates the receptor responses in the stretch receptor neurons of the crayfish. *Pflugers Arch - Eur J Physiol*. 2011; 462: 821-834. <https://doi.org/10.1007/s00424-011-1019-1>.
7. Purali, N. Fast calcium transients translate the distribution and conduction of neural activity in different regions of a single sensory neuron. *Invert Neurosci*. 2017; 17: 7. <https://doi.org/10.1007/s10158-017-0201-3>.
8. Coskun, C., Purali, N. Cloning and molecular characterization of a putative voltage-gated sodium channel gene in the crayfish. *Invert Neurosci*. 2016; 16: 2. <https://doi.org/10.1007/s10158-016-0185-4>.
9. Ergin, B., Purali, N. Cloning of a putative sodium/calcium exchanger gene in the crayfish. *Invert Neurosci*. 2018; 18: 9. <https://doi.org/10.1007/s10158-018-0213-7>.
10. Ergin, B., Saglam, B., Taskiran, E.Z., Bastug, T., Purali, N. *De novo* cloning and functional characterization of potassium channel genes and proteins in the crayfish *Astacus leptodactylus* (Eschscholtz, 1823) (Decapoda: Astacidea: Astacidae), *Journal of Crustacean Biology*. 2022; 42: 1 <https://doi.org/10.1093/jcbiol/ruac018>
11. Coşkun Jihad, N. Cloning of *Astacus Leptodactylus* Ryanodine Receptor Gene. MSc Thesis, Hacettepe University. Ankara, 2022.
12. Arslan, K., Saglam, B., Beyatli, N. C., Taskiran, E. Z., Bastug, T., & Purali, N. Cloning and functional characterization of a TMC-like channel gene and protein in the crayfish *Astacus leptodactylus* (Eschscholtz, 1823) (Decapoda: Astacidea: Astacidae). *Journal of Crustacean Biology*. 2023; 43(2) ruad032.
13. Ergin, B., Saglam, B., Arslan, K., Coskun Beyatli, N., Taskiran, Z.E., Bastug T, Purali N. *De novo* cloning and functional characterization of a

- mechanosensitive piezo-like ion channel in the crayfish. *Journal of Crustacean Biology*. 2023 (submitted)
14. Tyson, J.R. and Snutch, T.P. Molecular nature of voltage-gated calcium channels: structure and species comparison. *WIREs Membr Transp Signal*. 2013; 2: 181-206. <https://doi.org/10.1002/wmts.91>
 15. Zong, S., Zhou, J., Tanabe, T. Molecular determinants of calcium-dependent inactivation in cardiac L-type calcium channels. *Biochem Biophys Res Commun*. 1994; 201(3):1117-23. doi: 10.1006/bbrc.1994.1821. PMID: 8024553.
 16. Hille, B. Ion Channels of Excitable Membranes. *Sinauer Associates Inc*. 2001; 3rd Edition, Sunderland.
 17. Parent, L., Gopalakrishnan, M. Glutamate substitution in repeat IV alters divalent and monovalent cation permeation in the heart Ca²⁺ channel. *Biophys J*. 1995; 69(5):1801-1813. doi: 10.1016/S0006-3495(95)80050-0.
 18. Dolphin, A. C. A short history of voltage-gated calcium channels. *British journal of pharmacology*. 2006; 147: 56-62. <https://doi.org/10.1038/sj.bjp.0706442>
 19. Fatt, P. and Katz, B. The electrical properties of crustacean muscle fibres. *The Journal of physiology*. 1953; 120(1-2):171-204. <https://doi.org/10.1113/jphysiol.1953.sp004884>
 20. Schneider, M., Chandler, W. Voltage Dependent Charge Movement in Skeletal Muscle: A Possible Step in Excitation–Contraction Coupling. *Nature*. 1973; 242: 244-246. <https://doi.org/10.1038/242244a0>
 21. Catacuzzeno L, Franciolini, F. The 70-year search for the voltage-sensing mechanism of ion channels. *J Physiol*. 2022; 600: 3227-3247. <https://doi.org/10.1113/JP282780>
 22. Hagiwara, S., Byerly, L. Calcium channel. *Annu Rev Neurosci*. 1981; 4:69-125. doi: 10.1146/annurev.ne.04.030181.000441. PMID: 6261668.
 23. Tsien, R.W., Barrett, C.F. A Brief History of Calcium Channel Discovery. In: Voltage-Gated Calcium Channels. *Molecular Biology Intelligence Unit. Springer*. 2005. https://doi.org/10.1007/0-387-27526-6_3
 24. Borsetto, M., Barhanin, J., Fosset, M., Lazdunski, M. The 1,4-dihydropyridine receptor associated in the skeletal muscle voltage-dependent Ca²⁺ channel. *J Biol Chem*. 1985; 260:1 4255-14263.
 25. Hagiwara, S., Ozawa, S., Sand, O. Voltage clamp analysis of two inward current mechanisms in the egg cell membrane of a starfish. *J Gen Physiol*. 1975; 65(5):617-44. doi: 10.1085/jgp.65.5.617. PMID: 240906; PMCID: PMC2214882.
 26. Carbone, E., Lux, H. A low voltage-activated, fully inactivating Ca channel in vertebrate sensory neurones. *Nature*. 310; 501-502 (1984). <https://doi.org/10.1038/310501a0>
 27. Fedulova, S. A., Kostyuk, P. G., Veselovsky, N. S. Two types of calcium channels in the somatic membrane of new-born rat dorsal root ganglion neurones. *The Journal of physiology*. 1958; 359:431-446. <https://doi.org/10.1113/jphysiol.1958.sp015594>

28. Hess, P., Lansman, J.B., Tsien, R.W. Different modes of Ca channel gating behaviour favoured by dihydropyridine Ca agonists and antagonists. *Nature*. 1984; 311(5986):538-44. doi: 10.1038/311538a0. PMID: 6207437.
29. Catterall, W.A. Structure and regulation of voltage-gated Ca²⁺ channels. *Annu Rev Cell Dev Biol*. 2000; 16:521-555. doi: 10.1146/annurev.cellbio.16.1.521. PMID: 11031246.
30. Dolphin, A.C. Beta subunits of voltage-gated calcium channels. *Journal of bioenergetics and biomembranes*. 2003; 35:599-620. doi:10.1023/b:jobb.0000008026.37790.5a
31. Stephens, R. F., Guan, W., Zhorov, B. S., Spafford, J. D. Selectivity filters and cysteine-rich extracellular loops in voltage-gated sodium, calcium, and NALCN channels. *Frontiers in physiology*. 2015; 6:153. <https://doi.org/10.3389/fphys.2015.00153>
32. Mikami, A., Imoto, K., Tanabe, T., Niidome, T., Mori, Y., Takeshima, H., Narumiya, S., Numa, S. Primary structure and functional expression of the cardiac dihydropyridine-sensitive calcium channel. *Nature*. 1989; 340(6230): 230-233. <https://doi.org/10.1038/340230a0>
33. Ertel, E. A., Campbell, K. P., Harpold, M. M., Hofmann, F., Mori, Y., Perez-Reyes, E., Schwartz, A., Snutch, T. P., Tanabe, T., Birnbaumer, L., Tsien, R. W., Catterall, W. A. Nomenclature of voltage-gated calcium channels. *Neuron*. 2000; 25(3), 533-535. [https://doi.org/10.1016/s0896-6273\(00\)81057-0](https://doi.org/10.1016/s0896-6273(00)81057-0)
34. Catterall, W. A., Lenaeus, M. J., Gamal El-Din, T. M. Structure and Pharmacology of Voltage-Gated Sodium and Calcium Channels. *Annual review of pharmacology and toxicology*, 2020; 60: 133-154. <https://doi.org/10.1146/annurev-pharmtox-010818-021757>
35. Mori, Y., Friedrich, T., Kim, MS., Mikami, A., Nakai, J., Ruth, P., Bosse, E., Hofmann, F., Flockerz, V., Furuichi, T., Mikoshiba, K., Imoto, K., Tanabe, T., Numa, S. Primary structure and functional expression from complementary DNA of a brain calcium channel. *Nature*. 1991; 350: 398-402. <https://doi.org/10.1038/350398a0>
36. Dubel, S.J., Starr, T.V., Hell, J., Ahljianian, M.K., Enyeart, J.J., Catterall, W.A., Snutch, T.P. Molecular cloning of the alpha-1 subunit of an omega-conotoxin-sensitive calcium channel. *PNAS*. 1992; 89(11): 5058-5062. <https://doi.org/10.1073/pnas.89.11.5058>
37. Soong, T.A., Stea, A., Hodson, C.D., Dubel, S.J., Vincent, S.R., Snutch, T.P. Structure and Functional Expression of a Member of the Low Voltage-Activated Calcium Channel Family. *Science*. 1993; 260: 1133-1136. DOI: [10.1126/science.8388125](https://doi.org/10.1126/science.8388125)
38. Perez-Reyes E. Molecular physiology of low-voltage-activated t-type calcium channels. *Physiological reviews*, 2003; 83(1): 117-161. <https://doi.org/10.1152/physrev.00018.2002>

39. Catterall, W., Wisedchaisri, G., Zheng, N. The chemical basis for electrical signaling. *Nat Chem Biol.* 2017; **13**: 455–463. <https://doi.org/10.1038/nchembio.2353>
40. Yang, J., Ellnor, P., Sather, W.A., Zhang, J.F., Tsien R.W. Molecular determinants of Ca²⁺ selectivity and ion permeation in L-type Ca²⁺ channels. *Nature.* 1993; **366**: 158-161. <https://doi.org/10.1038/366158a0>
41. Heinemann, S.H., Terlau, H., Stühmer, W., Imoto, K., Numa, S. Calcium channel characteristics conferred on the sodium channel by single mutations. *Nature.* 1992; **356**(6368): 41-443.
42. Sather, W. A., McCleskey, E. W. Permeation and selectivity in calcium channels. *Annual review of physiology*, 2003; **65**: 133-159. <https://doi.org/10.1146/annurev.physiol.65.092101.142345>
43. Tang, L., Gamal El-Din, T. M., Payandeh, J., Martinez, G. Q., Heard, T. M., Scheuer, T., Zheng, N., Catterall, W. A. Structural basis for Ca²⁺ selectivity of a voltage-gated calcium channel. *Nature.* 2014; **505**(7481): 56-61. <https://doi.org/10.1038/nature12775>
44. Abderemane-Ali, F., Findeisen, F., Rossen, N. D., Minor, D. L. Jr. A Selectivity Filter Gate Controls Voltage-Gated Calcium Channel Calcium-Dependent Inactivation. *Neuron.* 2019; **101**(6): 1134-1149.e3. <https://doi.org/10.1016/j.neuron.2019.01.011>
45. Hering, S., Berjukow, S., Sokolov, S., Marksteiner, R., Weiss, R. G., Kraus, R., Timin, E. N. Molecular determinants of inactivation in voltage-gated Ca²⁺ channels. *The Journal of physiology.* 2000; **528**: 237-249. <https://doi.org/10.1111/j.1469-7793.2000.t01-1-00237.x>
46. Babich, O., Matveev, V., Harris, A. L., Shirokov, R. Ca²⁺-dependent inactivation of CaV1.2 channels prevents Gd³⁺ block: does Ca²⁺ block the pore of inactivated channels?. *The Journal of general physiology.* 2007; **129**(6): 477-483. <https://doi.org/10.1085/jgp.200709734>
47. Shaya, D., Findeisen, F., Abderemane-Ali, F., Arrigoni, C., Wong, S., Nurva, S. R., Loussouarn, G. Minor, D. L. Jr., Structure of a prokaryotic sodium channel pore reveals essential gating elements and an outer ion binding site common to eukaryotic channels. *Journal of molecular biology.* 2014; **426**(2): 467-483. <https://doi.org/10.1016/j.jmb.2013.10.010>
48. Beam, K., Adams, B., Niidome, T., Numa, S., Tanabe, T. Function of a truncated dihydropyridine receptor as both voltage sensor and calcium channel. *Nature.* 1992; **360**:169-171. <https://doi.org/10.1038/360169a0>
49. Wu, J., Yan, Z., Li, Z., Yan, C., Lu, S., Dong, M., Yan, N. Structure of the voltage-gated calcium channel Cav1.1 complex. *Science.* 2015; **350**:6267 <https://doi.org/10.1126/science.aad2395>

50. Tuluc, P., Yarov-Yarovoy, V., Benedetti, B., Flucher, B.E. Molecular Interactions in the Voltage Sensor Controlling Gating Properties of CaV Calcium Channels. *Structure*. 2016; 24(2):261-271. <https://doi.org/10.1016/j.str.2015.11.011>
51. Noda, M., Shimizu, S., Tanabe, T., Takai, T., Kayano, T., Ikeda, T., Takahashi, H., Nakayama, H., Kanaoka, Y., Minamino, N. Primary structure of *Electrophorus electricus* sodium channel deduced from cDNA sequence. *Nature*. 1984; 312(5990): 121-127. <https://doi.org/10.1038/312121a0>
52. Gurdon, J., Lane, C., Woodland, H., Marbaix, G. Use of Frog Eggs and Oocytes for the Study of Messenger RNA and its Translation in Living Cells. *Nature*. 1971; 233: 177-182. <https://doi.org/10.1038/233177a0>
53. Lin-Moshier, Y., Marchant, J. S. The *Xenopus* oocyte: a single-cell model for studying Ca²⁺ signaling. *Cold Spring Harbor protocols*. 2013; 3, 10.1101/pdb.top066308 [pdb.top066308. https://doi.org/10.1101/pdb.top066308](https://doi.org/10.1101/pdb.top066308)
54. Lin-Moshier, Y., Marchant, J. S. Nuclear microinjection to assess how heterologously expressed proteins impact Ca²⁺ signals in *Xenopus* oocytes. *Cold Spring Harbor protocols*. 2013; (3), 10.1101/pdb.prot072785 [pdb.prot072785. https://doi.org/10.1101/pdb.prot072785](https://doi.org/10.1101/pdb.prot072785)
55. Maldifassi, M. C., Wongsamitkul, N., Baur, R., Sigel, E. *Xenopus* Oocytes: Optimized Methods for Microinjection, Removal of Follicular Cell Layers, and Fast Solution Changes in Electrophysiological Experiments. *Journal of visualized experiments: JoVE*. 2016; 118: 55034. <https://doi.org/10.3791/55034>
56. Marchant J. S. Heterologous Protein Expression in the *Xenopus* Oocyte. *Cold Spring Harbor protocols*. 2018; (4), [pdb.prot096990. https://doi.org/10.1101/pdb.prot096990](https://doi.org/10.1101/pdb.prot096990)
57. Stühmer, W., Parekh, A.B. Electrophysiological Recordings from *Xenopus* Oocytes. In: *Sakmann, B., Neher, E. (eds) Single-Channel Recording*. Springer. 1995; https://doi.org/10.1007/978-1-4419-1229-9_15
58. Dumont, J.N. Oogenesis in *Xenopus laevis* (Daudin). I. Stages of oocyte development in laboratory maintained animals. *J. Morphol.* 1972; 136: 153-179. <https://doi.org/10.1002/jmor.1051360203>
59. Bocquet, N., Prado de Carvalho, L., Cartaud, J., Neyton, J., Le Poupon, C., Taly, A., Grutter, T., Changeux, J.P., Corringer, P.J. A prokaryotic proton-gated ion channel from the nicotinic acetylcholine receptor family. *Nature*. 2007; 445: 116-119 (2007). <https://doi.org/10.1038/nature05371>
60. MaksaeV, G., Haswell, E.S. Expression and characterization of the bacterial mechanosensitive channel MscS in *Xenopus laevis* oocytes. *J Gen Physiol*. 2011; 138 (6): 641-649. doi: <https://doi.org/10.1085/jgp.201110723>

61. Ottolia, M., John, S., Ren, X., Philipson, K.D. Fluorescent Na⁺-Ca⁺ Exchangers: Electrophysiological and Optical Characterization. *Journal of Biological Chemistry*. 2007; 282: 3695-3701. <https://doi.org/10.1074/jbc.M610425200>.
62. Wu, M., Gerhart, J. Chapter 1 Raising *Xenopus* in the Laboratory. *Methods in Cell Biology*. 1991; 36: 3-18. [https://doi.org/10.1016/S0091-679X\(08\)60269-1](https://doi.org/10.1016/S0091-679X(08)60269-1).
63. Elsner, H.A., Honck, H., Willmann, F., Kreienkamp, H., Iglauer, F. Poor quality of oocytes from *Xenopus laevis* used in laboratory experiments: prevention by use of antiseptic surgical technique and antibiotic supplementation. *Comp Med*. 2000; 50: 206-211.
64. Zhao, Y., Huang, G., Wu, J., Wu, Q., Gao, S., Yan, Z., Lei, J., Yan, N. Molecular Basis for Ligand Modulation of a Mammalian Voltage-Gated Ca²⁺ Channel. *Cell*. 2019; 177(6): 1495–1506.e12. <https://doi.org/10.1016/j.cell.2019.04.043>
65. Hockerman, G.H., Johnson, B. D., Abbott, M. R., Scheuer, T., Catterall, W. A. Molecular determinants of high affinity phenylalkylamine block of L-type calcium channels in transmembrane segment III_{S6} and the pore region of the alpha1 subunit. *The Journal of biological chemistry*. 1997; 272(30): 18759–18765. <https://doi.org/10.1074/jbc.272.30.18759>
66. Zamponi, G. W. Targeting voltage-gated calcium channels in neurological and psychiatric diseases. *Nature reviews. Drug discovery*. 2016; 15(1): 19–34. <https://doi.org/10.1038/nrd.2015.5>
67. Tang, L., Gamal El-Din, T. M., Swanson, T. M., Pryde, D. C., Scheuer, T., Zheng, N., & Catterall, W. A. (2016). Structural basis for inhibition of a voltage-gated Ca²⁺ channel by Ca²⁺ antagonist drugs. *Nature*. 2017; 537(7618): 117–121. <https://doi.org/10.1038/nature19102>
68. Gurkoff, G., Shahlaie, K., Lyeth, B., Berman, R. Voltage-gated calcium channel antagonists and traumatic brain injury. *Pharmaceuticals*. 2013; 6(7): 788–812. <https://doi.org/10.3390/ph6070788>
69. Moreno Davila, H. Molecular and functional diversity of voltage-gated calcium channels. *Annals of the New York Academy of Sciences*. 1999; 868: 102–117. <https://doi.org/10.1111/j.1749-6632.1999.tb11281.x>
70. Pinzi, L., Rastelli, G. Molecular Docking: Shifting Paradigms in Drug Discovery. *International journal of molecular sciences*. 2019; 20(18): 4331. <https://doi.org/10.3390/ijms20184331>
71. Forli, S., Huey, R., Pique, M., Sanner M.F., Goodsell, D.S., Olson, A.J. Computational protein–ligand docking and virtual drug screening with the AutoDock suite. *Nat Protoc*. 2016; 11: 905–919. <https://doi.org/10.1038/nprot.2016.051>
72. Cosconati, S., Forli, S., Perryman, A. L., Harris, R., Goodsell, D. S., Olson, A. J. Virtual Screening with AutoDock: Theory and Practice. *Expert opinion on drug*

- discovery*. 2010; 5(6): 597–607.
<https://doi.org/10.1517/17460441.2010.484460>
73. Chaudhary, K.K., Mishra, N. A Review on Molecular Docking: Novel Tool for Drug Discovery. *JSM Chem*. 2016; 4(3): 1029.
 74. U.S. National Library of Medicine. (n.d.). *Polymerase chain reaction (PCR)*. National Center for Biotechnology Information. Retrieved November 21, 2021, from <https://www.ncbi.nlm.nih.gov/probe/docs/techpcr/>
 75. Chuang, L.Y., Cheng, Y.H., Yang, C.H. Specific primer design for the polymerase chain reaction. *Biotechnol Lett*. 2013; 35(10): 1541-1549. doi:10.1007/s10529-013-1249-8
 76. The MathWorks, Inc. (2021). *MATLAB version: 9.11.0.1769968 (R2021b)*. Available: <https://www.mathworks.com>.
 77. Altschul, S.F., Gish, W., Miller, W., Myers, E.W. & Lipman, D.J. "Basic local alignment search tool." *J. Mol. Biol.* 1990; 215: 403-410.
 78. Shennan Lu et al. "*CDD/SPARCLE: the conserved domain database in 2020.*", *Nucleic Acids Res.* 2020;48(D1)265-8.
 79. Wu, J., Yan, Z., Li, Z., Qian, X., Lu, S., Dong, M., Zhou, Q., Yan, N. Structure of the voltage-gated calcium channel Ca_v1.1 at 3.6 Å resolution. *Nature*. 2016; 537: 191–196. <https://doi.org/10.1038/nature19321>.
 80. Isaev, D., Solt, K., Gurtovaya, O., Reeves, J. P., Shirokov, R. Modulation of the voltage sensor of L-type Ca²⁺ channels by intracellular Ca²⁺. *The Journal of general physiology*. 2004; 123(5): 555-571. <https://doi.org/10.1085/jgp.200308876>
 81. Purali, N. Fast calcium transients translate the distribution and conduction of neural activity in different regions of a single sensory neuron. *Invert Neurosci*. 2017; 17: 7. <https://doi.org/10.1007/s10158-017-0201-3>.
 82. Waterhouse, A., Bertoni, M., Bienert, S., Studer, G., Tauriello, G., Gumienny, R., Heer, F.T., de Beer, T.A.P., Rempfer, C., Bordoli, L., Lepore, R., Schwede, T. SWISS-MODEL: homology modelling of protein structures and complexes. *Nucleic Acids Research*, 2018; 46: W296–W303.
 83. Humphrey, W., Dalke, A. & Schulten, K. VMD-visual molecular dynamics. *Journal of Molecular Graphics*. 1996; 14: 33–38.
 84. Nugent, T., Jones, D.T. Membrane protein orientation and refinement using a knowledge-based statistical potential. *BMC Bioinformatics*. 2013; 14:276. doi: 10.1186/1471-2105-14-276.
 85. Bibollet, H., Kramer, A., Bannister, R.A., Hernández-Ochoa, E.O. Advances in Ca_v1.1 gating: New insights into permeation and voltage-sensing mechanisms. *Channels*. 2023; 17(1): 2167569. <https://doi.org/10.1080/19336950.2023.2167569>

8. APPENDIX

Appendix 1: Thesis Originality Report

Berk SAĞLAM-PhD

ORJİNALLİK RAPORU

% 20	% 15	% 10	% 5
BENZERLİK ENDEKSİ	İNTERNET KAYNAKLARI	YAYINLAR	ÖĞRENCİ ÖDEVLERİ

BİRİNCİL KAYNAKLAR

1	openaccess.hacettepe.edu.tr:8080 İnternet Kaynağı	% 7
2	bmcdevbiol.biomedcentral.com İnternet Kaynağı	% 1
3	www.biorxiv.org İnternet Kaynağı	% 1
4	Terunao Takahara, Shin-ichi Kanazu, Shuichi Yanagisawa, Hiroshi Akanuma. " Heterogeneous Sp1 mRNAs in Human HepG2 Cells Include a Product of Homotypic Splicing ", Journal of Biological Chemistry, 2000 Yayın	% 1
5	Annette C Dolphin. "A short history of voltage-gated calcium channels", British Journal of Pharmacology, 01/2006 Yayın	<% 1
6	molecular-cancer.biomedcentral.com İnternet Kaynağı	<% 1
7	www.seaskybio.com İnternet Kaynağı	<% 1

Appendix 2: Digital Receipt



Dijital Makbuz

Bu makbuz ödevinizin Turnitin'e ulaştığını bildirmektedir. Gönderiminize dair bilgiler şöyledir:

Gönderinizin ilk sayfası aşağıda gönderilmektedir.

Gönderen: Berk Sağlam
Ödev başlığı: Berk Sağlam_PhD_final
Gönderi Başlığı: Berk SAĞLAM-PhD
Dosya adı: tez_son_turnitin.docx
Dosya boyutu: 3.11M
Sayfa sayısı: 45
Kelime sayısı: 8,373
Karakter sayısı: 56,167
Gönderim Tarihi: 02-Ağu-2023 11:36ÖÖ (UTC+0300)
Gönderim Numarası: 2140346924

1. INTRODUCTION

Voltage-gated calcium channels (Ca_v), gated by potential changes in the cell membrane, generate a Ca²⁺ influx acting as a second messenger for many important cellular processes like muscle activity, secretion, and gene transcription [1].

Aistacus leptodactylus is a very useful model animal for many types of experiments. Due to the simplified morphology and relative ease in access to the neural circuitry it is particularly convenient for many neuroscience studies. The electrical and functional properties of the many types of cells almost have completely been investigated. [2-7]. In comparison to the functional studies amount of information about the genetic properties of the animal is rather limited. Recently, several ion channel genes that give cells many essential electrical and functional properties have been explored by our laboratory. mRNAs coding a voltage-gated sodium channel, sodium-calcium exchanger, inward-rectifier potassium channel, calcium-activated potassium channel, ryanodine receptor, transmembrane channel-like protein and Piezo channel have been cloned [8-13]. Calcium channels play an important role in the muscle and neural physiology in this model animal. However, there is no information about the genetic and molecular properties of the voltage-gated calcium channels in this model animal.

Therefore, the aim of this study was to clone the voltage-gated calcium channel (Ca_v) of *Aistacus leptodactylus* and to examine its electrical and functional properties by computational modeling and heterologous expressing in *Xenopus laevis* oocytes.

9. CURRICULUM VITEA